

1 ~~Pelagic~~Coccolithophore abundance and production and their impacts on

2 **particulate inorganic carbon cycling in the western North Pacific**

3 Yuye Han^{1,2}, Zvi Steiner², Zhimian Cao^{1*}, Di Fan³, Junhui Chen¹, Jimin Yu³ and Minhan Dai^{1*}

4 ¹State Key Laboratory of Marine Environmental Science & College of Ocean and Earth Sciences, Xiamen University, Xiamen,

5 China

6 ²Marine Biogeochemistry Division, GEOMAR Helmholtz Centre for Ocean Research, Kiel, Germany

7 ³Laoshan Laboratory, Qingdao, China

8

9 *Correspondence to:* mdai@xmu.edu.cn & zmcao@xmu.edu.cn

Abstract. Coccolithophores ~~are globally a type of single-celled phytoplankton that is~~ abundant ~~single-celled and shelled~~ phytoplankton that play an important role in the marine carbon cycle due to their contribution to the carbonate pump in global oceans, are closely associated with the carbonate pump and thus play a crucial role in the marine carbon cycle. However, the current distribution of coccolithophore species and their dependence on environmental conditions are poorly known, hindering our ability to predict the response of the marine carbonate pump to changing climates. Here we investigated coccolithophore abundances, species compositions, coccolithophore calcium carbonate (CaCO_3 as calcite) and particulate inorganic carbon (PIC) concentrations in the upper water column of the western North Pacific Ocean, along a meridional transect spanning the oligotrophic subtropical gyre and the nutrient-rich Kuroshio-Oyashio transition region. Our ~~results-samples and data~~ revealed that *Umbellosphaera tenuis* was the ~~numerically~~ dominant coccolithophore species in the ~~former~~ subtropical gyre, while *Emiliania huxleyi* and *Syracosphaera* spp. dominated in the ~~transition region~~ latter. The coccolithophore community composition showed significant depth- and latitude-dependent variations. Calcite from coccolithophores accounted for an average of $79 \pm 27\%$ of the CaCO_3 standing stock in Niskin bottle samples in the euphotic zone, with a higher contribution observed in the subtropical gyre ($91 \pm 30\%$) compared to the Kuroshio-Oyashio transition region ($70 \pm 24\%$). This pattern was further supported by size-fractionated PIC concentrations of in situ pump samples, which showed a greater contribution of small PIC to total PIC in the subtropical gyre ($76 \pm 11\%$) than in the transition region ($67 \pm 13\%$). During the sampling period, coccolithophore CaCO_3 production rate ranged from 0.8 to $2.1 \text{ mmol m}^{-2} \text{ d}^{-1}$, averaging $1.5 \pm 0.7 \text{ mmol m}^{-2} \text{ d}^{-1}$ in the subtropical gyre and $1.2 \pm 0.4 \text{ mmol m}^{-2} \text{ d}^{-1}$ in the transition region. Coccolithophore calcite contributed a major fraction of the PIC standing stocks above a depth of 150 m , among which *E. huxleyi* was the most important producer while less abundant and larger species also played a role. The coccolithophore CaCO_3 production rate in the subtropical gyre ($0.62 \text{ mol m}^{-2} \text{ yr}^{-1}$) was ~ 5 -fold higher than that in the Kuroshio-Oyashio transition region ($0.14 \text{ mol m}^{-2} \text{ yr}^{-1}$), indicating that inorganic carbon metabolism driven by coccolithophores is relatively strong in oligotrophic ocean waters. Using a box model including coccolithophore CaCO_3 production and metabolic calcite saturation state, we demonstrated that CaCO_3 dissolution associated with organic carbon metabolism can generate excess alkalinity in the oversaturated upper water column of the western North Pacific Ocean. Results of our study highlight the critical role of coccolithophores in the pelagic CaCO_3 production and dissolution cycle, particularly in oligotrophic ocean waters; knowledge of these processes is important to assess PIC cycling.

35 ~~and carbonate pump efficiency in the pelagic ocean.~~

36

1 Introduction

Calcium carbonate (CaCO_3) production and dissolution ~~comprise two major processes associated with~~ CaCO_3 cycling in the ocean, and ~~are~~ a key component of the global oceanic carbon cycle (Broecker and Peng, 1982) ~~via the so-called~~ through the carbonate pump (Volk and Hoffert, 1985). Production of biogenic CaCO_3 by calcifying plankton in the euphotic zone elevates the partial pressure of carbon dioxide (CO_2) in seawater (e.g., Feely et al., 2002), while ballasting of sinking particles can promote the transport of carbon from the surface to deep sea and marine sediments (e.g., Armstrong et al., 2001; Klaas and Archer, 2002). Dissolution of CaCO_3 in the water column acts as a buffer to facilitate ocean sequestration of atmospheric CO_2 and ~~has the effect of reducing~~ reduces the rate of ocean acidification (Feely et al., 2004; Barrett et al., 2014). Over the last decade, ocean acidification, a global reduction in seawater pH caused by the uptake of anthropogenic CO_2 , has emerged as a significant feedback mechanism. This acidification feedback mechanism makes making it harder for calcifying organisms to produce their skeletons, and thus adversely affects marine ecosystems (Feely et al., 2004; Ma et al., 2023)(Feely et al., 2004; Steiner et al., 2018). Therefore, quantification of marine CaCO_3 production and dissolution is of vital importance in determining the response of marine ecosystems to changes in the partial pressure of CO_2 .

Marine CaCO_3 occurs in the form of calcite, aragonite and high-magnesium calcite. Coccolithophores are a key, single-celled phytoplankton taxonomic group, responsible for a large percentage (30–60 %) of modern oceanic CaCO_3 production and 10–20 % of marine primary production on a global scale (Poulton et al., 2006, 2013). Coccolithophore calcite accounts for a major fraction (24–80 %) of the CaCO_3 exported to the deep sea and sediments (Broerse et al., 2000; Young and Ziveri, 2000; Rigual Hernández et al., 2020). ~~Field observations~~Data assessment along a northeast Pacific transect from Hawaii to Alaska suggested that coccolithophore calcite comprises 90 % of the total CaCO_3 production in the euphotic zone, while pteropods and foraminifera only play a minor role (Ziveri et al., 2023). However, large uncertainties remain in estimates of the production rate of CaCO_3 in the upper ocean, as well as the contributions of different plankton groups, which are still unclear and vary across regions (Balch et al., 2007; Berelson et al., 2007; Smith and Mackenzie, 2016; Ziveri et al., 2023). Based on a global compilation of CaCO_3 production using in situ ^{14}C incubations, Daniels et al. (2018) found that calcification rate ranged from ~~40–0.1 to 600–6 mg-mmol~~ $\text{m}^{-2} \text{d}^{-1}$ in the euphotic zone. A recent estimate of CaCO_3 biomass from three main pelagic calcifying plankton groups also suggested large variation in CaCO_3 production in the eastern North Pacific Ocean,

ranging from 140 to 729 mg l.l to 7.3 mmol m⁻² d⁻¹ (Ziveri et al., 2023). ~~The generally low coverage of observations and the considerable spatiotemporal variation shown by available data, along with the current scarcity of studies, most likely result in deviations among regional estimates.~~

CaCO₃ dissolution is generally assumed to mainly occur below the saturation horizon. However, this assumption has been challenged by an increasing number of studies which suggest considerable dissolution in the oversaturated upper water column where CaCO₃ saturation state (Ω) is greater than 1 (Sabine et al., 2002; Chung et al., 2003; Berelson et al., 2007; Barrett et al., 2014). Shallow water CaCO₃ dissolution is supported by excess alkalinity/calcium (Feely et al., 2002, 2004; Cao and Dai, 2011; Subhas et al., 2022), decreased sinking fluxes of particulate inorganic carbon (PIC) measured using the ²³⁴Th method, and sediment trap data from the upper ocean (Dong et al., 2019; Roca-Martí et al., 2021). One possible mechanism for CaCO₃ dissolution in calcite oversaturated shallow waters is the dissolution of more soluble forms of CaCO₃ including aragonite pteropods and high-Mg fish calcites (Honjo et al., 2008; Wilson et al., 2009; Dong et al., 2019; Folkerts et al., 2024; Oehlert et al., 2024). An alternative hypothesis is that microbial oxidation of organic matter produces an acidic microenvironment conducive for carbonate dissolution (Bishop et al., 1980; Milliman et al., 1999). The digestive system of grazing zooplankton may also contain acidic conditions facilitating CaCO₃ dissolution (Pond et al., 1995; White et al., 2018).

The North Pacific Ocean is a vital region for modulating the carbon cycle, as it accounts for ~25 % of the global ocean sink for atmospheric CO₂ (Takahashi et al., 2009). In the eastern North Pacific Ocean, CaCO₃ production, export, and dissolution have been studied along a transect from Hawaii to Alaska (Dong et al., 2019, 2022; Naviaux et al., 2019; Subhas et al., 2022; Ziveri et al., 2023). ~~Ziveri et al. (2023) found which revealed that depth-integrated CaCO₃ production in the nutrient-rich subpolar gyre is twice as high as that in the nutrient-poor subtropical gyre. This contrast, however, is smaller than the sixfold to sevenfold difference based on satellite estimates of surface particulate inorganic carbon (PIC), indicating the importance of coccolithophore CaCO₃ production over a deeper euphotic zone in deep waters and the limitation of satellite products as highlighted by Neukermans et al. (2023). These investigations also suggested that widespread shallow water CaCO₃ dissolution is driven by metabolic activity along the Hawaii-to-Alaska transect.~~

Here, we determined the abundances and species compositions of coccolithophores, as well as the concentrations of coccolithophore calcite and PIC based on both Niskin bottle and in situ pump sampling in the upper water column of the

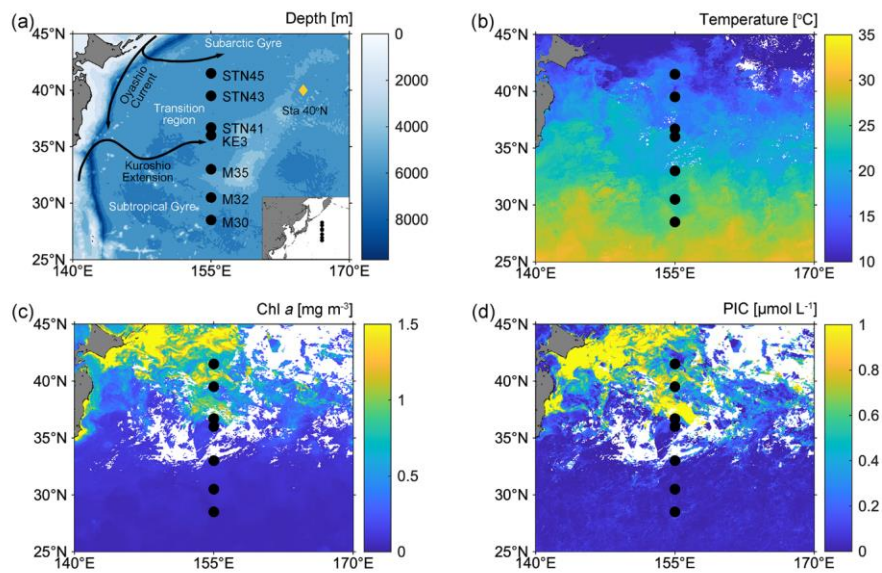
87 western North Pacific Ocean. Additionally, we conducted measurements of environmental conditions such as nutrient and
88 carbonate chemistry parameters. The aims of this research were to answer the following questions: (1) What is the distribution
89 of coccolithophore abundances and species compositions across the oligotrophic-nutrient replete environmental gradient? (2)
90 What is the contribution of coccolithophores to CaCO_3 production in the euphotic zone? ~~(3) Does shallow-water CaCO_3~~
91 ~~dissolution occur in the western North Pacific Ocean, and what is the significance of metabolic activities in driving dissolution~~
92 ~~in oversaturated ambient conditions?~~

94 **2 Methods**

95 **2.1 Sample collection**

96 Sampling was conducted onboard R/V *Tan Kah Kee* during cruise NORC2022-306 from 09 June to 25 July 2022. The cruise
97 trajectory crossed from the oligotrophic North Pacific Subtropical Gyre (NPSG) to the relatively nutrient-rich Kuroshio-
98 Oyashio transition region along the 155°E meridian (Fig. 1a; Table S1). Seven sampling stations can be divided into those
99 located in the NPSG region, including stations M30, M32 and M35, characterized by high sea-surface temperature (SST) and
100 low surface chlorophyll *a* (Chl *a*) and PIC concentrations, and those located in the Kuroshio-Oyashio transition region,
101 including stations KE3, STN41, STN43 and STN45, featuring lower SST, but higher Chl *a* and PIC concentrations (Fig. 1b–
102 d).

103



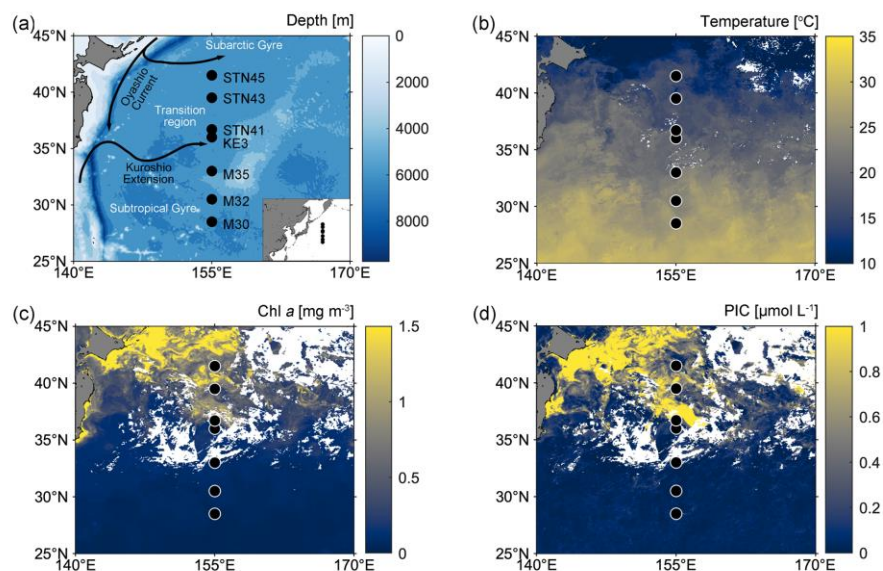


Fig 1. (a) Map of the western North Pacific Ocean showing sampling stations (black filled circles) and major surface currents (solid black lines). The yellow diamond indicates station 40° N at which particulate inorganic carbon (PIC) sinking flux was investigated by Honda et al., (2002); (b–d) satellite-based temperature, chlorophyll *a* (Chl *a*) and particulate inorganic carbon (PIC) concentrations in surface water from 1st to 30th June 2022 in June 2022 (data from the Moderate Resolution Imaging Spectroradiometer (MODIS)-Aqua satellite; <https://oceancolor.gsfc.nasa.gov/l3/>).

Water samples were collected within the water column above 300 m depth using Niskin bottles on a rosette system equipped with SBE-911 conductivity-temperature-depth (CTD) sensors (Sea-Bird Electronics, Inc., Bellevue, WA, USA). For PIC analyses, 24 L of seawater were collected using acid-cleaned fluorinated bottles and filtered through two quartz microfiber (QMA) filters (1.0 μm pore size, 25 mm diameter). For coccolithophore analyses, 2–4 L of seawater were collected and gently filtered through polycarbonate membranes (0.8 μm pore size, 25 mm diameter), using a vacuum pump at <20 mm Hg pressure.

~~Membrane F~~ilters were oven-dried at 60°C and stored in plastic petri dishes.

Size-fractionated particles were collected using McLane Research in situ pumps. Filter holders were loaded with a 51 µm Sefar polyester mesh prefilter followed by paired Whatman QMA filters. Hereafter, we refer to the two particle size fractions as large ($> 51\text{ }\mu\text{m}$) and small ($1\text{--}51\text{ }\mu\text{m}$) size fractions (~~(LSF, $> 51\text{ }\mu\text{m}$ and SSF, $1\text{--}51\text{ }\mu\text{m}$, respectively)~~). A 1/4 subsample of the 51 µm polyester mesh prefilter and two circles of 23 mm diameter subsample of the QMA filter were analyzed for ~~LSF-large~~ and ~~SSF-small~~ PIC concentrations, respectively, and the sum of the two fractions yielded the total PIC (~~PIC_{total}~~) concentration.

2.2 Sample analyses

PIC concentrations were determined by measuring the amount of CO₂ released after acid treatment of the filters using a Thermo Delta V Plus isotope ratio mass spectrometer (IRMS, Thermo Fisher, USA) coupled with a Thermo Gasbench II system at the Center for Isotope Geochemistry and Geochronology of the Laoshan Laboratory (Li et al., 2021). International reference materials of calcite NBS-18 and IAEA-603 were measured for calibration. The ~~PIC~~-analytical precision of PIC determination was ~~better than~~ $\leq 10\%$ (one standard deviation, 1SD).

~~A portion of the filters was~~Filters were cut and mounted with a carbon sticky tab on a stub and gold-coated prior to analysis using a Quanta 650 FEG field-emission scanning electron microscope (SEM). The coccosphere cell or detached coccolith concentrations (CC, cells or coccoliths L⁻¹) were estimated as follows:

$$CC = (F * C)/(V * S) \quad (1)$$

where F is the effective filtration area (336.9 mm²), C is the total number of coccosphere cells or detached coccoliths, V is the filtered seawater volume, and S is the total area of fields of view (mm²). This cell counting strategy gives a detection limit of at least 1.87 cells mL⁻¹ (Bollmann et al., 2002). The coccolithophore abundance in four samples, that were collected at 10 m and 200 m at station M30, 200 m at station KE3 and 200 m at station STN45, fell below the detection limit. Despite potential inaccuracies, these values are still meaningful as they indicate an exceptionally low coccolithophore presence. Coccolithophore species identification followed Young et al. (2003) and the Nannotax3 website (<http://ina.tmsoc.org/Nannotax3/>). Aggregates formed by clusters of multiple coccolithophores were quantified in terms of abundance but were excluded from the coccolithophore calcite calculations, mainly due to the difficulty in accurately determining the number of individual coccoliths within the aggregates. Individual coccolithophore calcite content was calculated by multiplying the number of coccoliths per

cell by the average coccolith calcite mass of a given species (Young and Ziveri, 2000; Yang and Wei, 2003; Boeckel and Baumann, 2008; Beuvier et al., 2019; Jin et al., 2022). All the biometry work based on SEM images was conducted using imageJ free software (imagej.nih.gov/ij/) and Coccobiom2-SEM measuring macro (Young, 2015). Individual coccolithophore calcite content was calculated by multiplying the number of coccoliths per cell by the average coccolith calcite mass of a given species. The average coccolith mass was estimated based on the coccolith size (usually using coccolith length) and a factor related to coccolith cross-sectional shape (Young and Ziveri, 2000):

$$m \text{ (pg CaCO}_3\text{)} = 2.7 * K_s * l^3 \quad (2)$$

where l is the coccolith size (μm), K_s is a species-specific shape constant, and 2.7 is the calcite density (CaCO_3 ; $\text{pg } \mu\text{m}^{-3}$). The specific coccolith distal shield length or process height used in the calculation was measured from SEM images. Measurements were conducted using ImageJ free software (imagej.nih.gov/ij/) and Coccobiom2-SEM measuring macro (Young, 2015). The K_s values used were from Young and Ziveri (2000) and Jin et al. (2016). The number of coccoliths per coccosphere was obtained from Yang and Wei (2003) and Boeckel and Baumann (2008). The calculation of coccolith PIC is detailed in Table S2 in the Supplement. Sheward et al. (2024) have extensively discussed the potential errors of the morphometric-based calcite estimation method, suggesting that an additional uncertainty of 5–40 % may arise from slight variations in K_s and size between coccoliths on the same coccosphere, as well as errors in coccolith number estimation. Additionally, it is important to note that further uncertainties can be introduced by counting inaccuracies, particularly in cases where clumps or overlapping coccoliths are present. Despite these possible errors and limitations, our data and results offer robust and comparable insights into coccolithophore calcite dynamics.

Chl *a* concentrations were measured after being extracted with 90 % acetone for 14 h at -20°C using a Trilogy Laboratory Fluorometer with non-acidification module (Turner Designs, USA) (Welschmeyer, 1994). Nutrient samples were collected in acid-washed Nalgene high-density polyethylene bottles and determined onboard the vessel using a Four-channel Continuous-Flow Technicon AA3 Autoanalyzer (Bran+Luebbe GmbH). The detection limits were $0.1 \mu\text{mol L}^{-1}$, $0.08 \mu\text{mol L}^{-1}$, and $0.16 \mu\text{mol L}^{-1}$ for dissolved inorganic nitrogen (DIN, nitrate plus nitrite), soluble reactive phosphate (SRP), and dissolved silicate (DSi), respectively. The analytical precisions (derived from repeat measurements of aged deep seawater) were 0.44% for DIN, 0.91% for SRP, and 0.28% for DSi ($n = 82$). Analysis of reference standard LOT.CM (KANSO TECHNOS CO., LTD.)

带格式的: 字体: 倾斜

带格式的: 字体: 倾斜, 下标

produced concentrations of $33.72 \pm 0.13 \mu\text{mol L}^{-1}$ for DIN, $2.460 \pm 0.025 \mu\text{mol L}^{-1}$ for SRP, and $102.2 \pm 0.3 \mu\text{mol L}^{-1}$ for DSI ($n = 20$), which agree well with consensus values (http://www.kanso.co.jp/eng/pdf/certificate_cb.pdf). For measurements of DIN and SRP concentrations in surface samples below the detection limit of the AA3 Autoanalyzer, duplicate samples were collected and frozen separately at -20°C until analysis. Nanomolar DIN concentrations were determined using a continuous-flow analysis system combined with a liquid waveguide capillary flow cell as described by Zhang (2000). The detection limit was 5.2 nmol L^{-1} and the analytical precision was 7.5% (derived from repeat measurements of aged deep seawater with 1000-fold dilution, $36.2 \pm 2.7 \text{ nmol L}^{-1}$, $n = 57$). Nanomolar SRP concentrations were measured using an automated analyzer including a syringe pump and multiposition selection valve combined with a solid-phase extraction cartridge (Deng et al., 2020). The detection limit was 2.5 nmol L^{-1} and the analytical precision was 5% (derived from repeat measurements of aged deep seawater with 1000-fold dilution, $26.0 \pm 1.2 \text{ nmol L}^{-1}$, $n = 56$). Seawater ammonium (NH_4^+) concentrations were measured onboard using solid-phase extraction combined with fluorescence determination with a detection limit of 3.6 nmol L^{-1} (Zhu et al., 2013, 2018).

Samples for analysis of dissolved inorganic carbon (DIC) and total alkalinity (TA) were collected in 250 mL PYREX® borosilicate glass bottles, and poisoned with 250 μL of a HgCl_2 -saturated solution upon sample collection. DIC was measured using an infrared CO_2 detector (Apollo ASC-3), with a precision of $\pm 2 \mu\text{mol L}^{-1}$ (Cai et al., 2004). TA was determined on 25 mL samples using an open-cell setting based on the Gran titration technique (Cai et al., 2010) with a Kloeckner digital syringe pump. The analytical precision was $\pm 2 \mu\text{mol L}^{-1}$. Both DIC and TA concentrations were calibrated against certified reference materials provided by Andrew G. Dickson (the Scripps Institution of Oceanography, University of California, San Diego, USA).

2.3 Estimation of CaCO_3 production rate

The euphotic zone bottom at each station was defined as the depth where surface photosynthetically active radiation (PAR) reaches 0.1 % (Table S1). CaCO_3 production rates ~~above 150 m in the euphotic zone~~ were determined by dividing measurements of the living CaCO_3 standing stock (which only included whole coccosphere cells and excluded loose coccoliths) by the coccolithophore turnover time, which is 0.7–10 days with a growth rate ranging from 0.1 to 1.5 cell divisions day^{-1} (Krumhardt et al., 2017; Ziveri et al., 2023). The coccolithophore turnover time was derived from both laboratory and field

estimates, as well as simulations from a generalized coccolithophore model, which has also been applied to the eastern North Pacific Ocean (Krumhardt et al., 2017; Ziveri et al., 2023). We are aware that different coccolithophore species exhibit widely varying growth rates and cell growth phase differs. Smaller cells produce fewer coccoliths during the exponential growth phase characterized by rapid division, whereas larger cells generate more coccoliths during the early stationary phase when cell division slows down (Raven and Crawford, 2012; Krumhardt et al., 2017). We also acknowledge that estimating coccolithophore calcite and production rates using an average coccolith calcite value introduces uncertainties, as this approach does not fully account for the complexity of coccolith dynamics, including rapid cycling and reabsorption (Johns et al., 2023). Despite these possible errors and uncertainties, our estimations generally comparable with those of prior work (e.g., Daniels et al., 2018), remain a reliable basis for assessing coccolithophore calcification. Uncertainty in the CaCO_3 standing stock estimates, which were obtained by vertically integrating PIC concentrations in the euphotic zone above a depth of 150 m, was typically $\pm 10\%$ (1SD).

A Monte Carlo-based probabilistic approach was used to determine the CaCO_3 production rate and the uncertainties associated with the turnover time using the R package *vioplot* a flat probability distribution in MATLAB visualized by a violin plot (Hoffmann, 2015). To obtain an annual CaCO_3 production based on our field observations, we used the ratio of satellite-derived PIC for July 2022 to annual climatology PIC (data from the NASA Goddard Space Flight Center's Ocean Ecology Laboratory) to calibrate for potential seasonal variability (Ziveri et al., 2023).

2.4 Influence of environmental conditions on coccolithophores

The redundancy analysis (RDA) is a widely used multivariate analytical method to identify relationships among individual variables in different categories. Prior to the RDA, statistical differences in environmental variables were evaluated using an analysis of variance (one-way ANOVA), while collinearity between environmental variables was accounted for by calculating variance inflation factors (VIF). Forward selection of variables was subsequently carried out until all VIF scores were <10 , in order to only including variables that are not significantly correlated. These criteria reduced the number of environmental variables used in the RDA. Monte Carlo permutation tests, based on 1000 randomizations, were performed to identify the most significant and independent effect on variation in the coccolithophore community composition. The overall significance of the explanatory variables after forward selection was evaluated through ANOVA ($\alpha < 0.05$) and coefficient of determination (r^2).

and adjusted r^2 were calculated to assess the power of a selected RDA model using the *vegan* package (Oksanen, 2010). The redundancy analysis (RDA) function in the *vegan* package in R, in combination with Monte Carlo permutation, were performed to assess the relative importance of environmental variables in explaining the overall variation in the composition of the coccolithophore community (Oksanen et al., 2007). The contribution of each environmental variable to community variation was determined by hierarchical partitioning in canonical analysis via the ‘dbRDA’ function in the ‘rdacca.hp’ package in R (Lai et al., 2022). We further conducted random forest analyses to identify the main predictors of coccolithophore abundance with the ‘randomForest’ package in R (Liaw and Wiener, 2002).

2.5 Evaluation of shallow water CaCO_3 dissolution

To estimate the effect of microenvironment undersaturation driven by microbial oxidation of organic matter, we assumed that aerobic metabolic activity of marine particles consumes all ambient oxygen and alters ambient dissolved inorganic carbon (DIC) and total alkalinity (TA). This process decreases microenvironment Ω and thus causes CaCO_3 dissolution. We calculated Ω due to in situ metabolism (defined as Ω_{met}) using the concurrently altered DIC, TA and soluble reactive phosphate (SRP) concentrations following Subhas et al., (2022):

$$\text{DIC}_{\text{met}} = \text{DIC} + [\text{O}_2] * R_{\text{CO}_2} \quad (2a)$$

$$\text{TA}_{\text{met}} = \text{TA} - [\text{O}_2] * R_{\text{NO}_3} \quad (2b)$$

$$\text{SRP}_{\text{met}} = \text{SRP} + [\text{O}_2] * R_{\text{PO}_4} \quad (2c)$$

where R_{CO_2} , R_{NO_3} and R_{PO_4} denote the Redfield ratio of carbon to oxygen (0.688), nitrate to oxygen (0.0941), and phosphate to oxygen (0.0059), respectively (Anderson and Sarmiento, 1994).

A one-dimensional (1-D) model was used to diagnose the sinking flux and CaCO_3 dissolution rate in the upper 1000 m of the water column by coccolithophore CaCO_3 production, coccolith dissolution kinetics and Ω_{met} (Dong et al., 2019; Subhas et al., 2022). The model assumes that dissolution of CaCO_3 particles occurs when the water column $\Omega_{\text{met}} < 1$. The magnitude of dissolution thus depends on the initial sinking flux, Ω_{met} and particle residence time as follows:

$$\text{Flux}_{z_i} = \text{Flux}_{z_{i-1}} * \left(1 - R_{\text{diss}} * \frac{z_i - z_{i-1}}{w} \right) \quad (3)$$

where Flux_{z_i} and $\text{Flux}_{z_{i-1}}$ ($\text{mmol m}^{-2} \text{d}^{-1}$) denote the CaCO_3 sinking flux at a given depth z_i and its overlying depth z_{i-1} .

241 respectively; R_{diss} ($\text{g g}^{-1} \text{d}^{-1}$) denotes CaCO_3 dissolution rate which is a function of the Ω_{sat} at depth $Z_{\text{d-1}}$ (Subhas et al., 2018;
242 Subhas et al., 2022) and w (m d^{-1}) denotes the particle sinking rate.

243 TA regeneration rate (R_{TA} , $\mu\text{mol kg}^{-1} \text{yr}^{-1}$) at depth Z_{d} resulting from shallow water CaCO_3 dissolution was calculated based
244 on the following equation:

245
$$R_{\text{TA},Z_{\text{d}}} = \frac{2 + F(\text{H}_2\text{SiO}_4) + R_{\text{diss}}}{\rho + w} \quad (4)$$

246 where ρ denotes the density of seawater (1029 kg m^{-3}).

248 3 Results

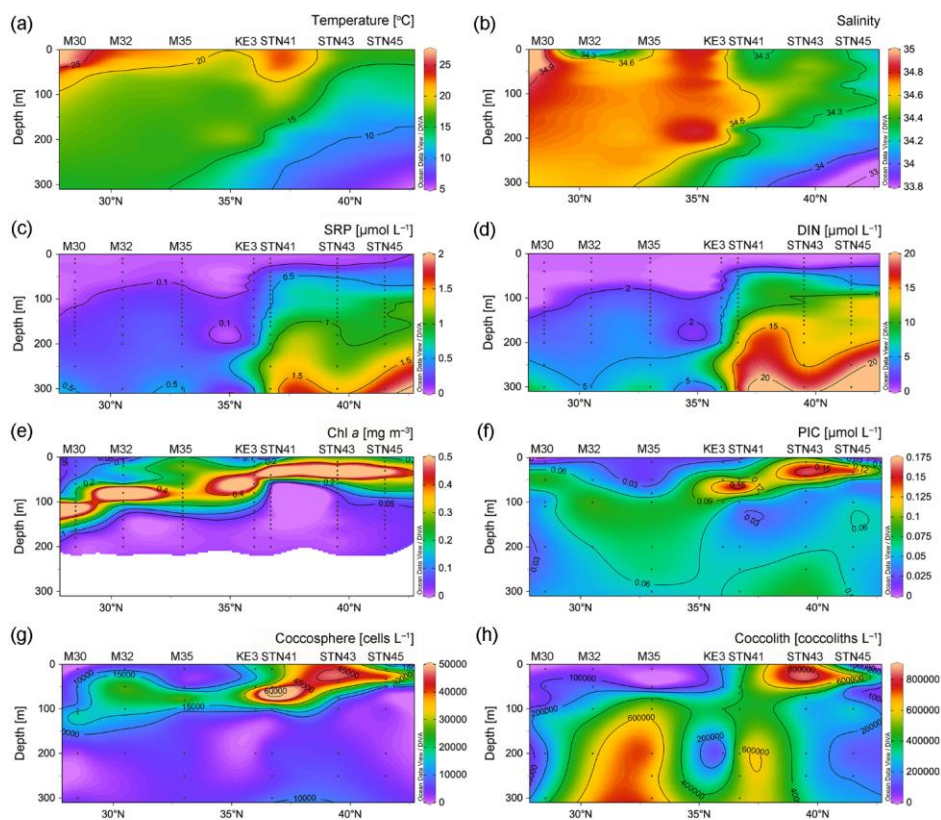
249 3.1 Hydrography and nutrient line

250 ~~Temperature and salinity were high in surface water and gradually decreased with increasing depth above 300 m.~~
251 Hydrochemical variables clearly exhibited a south to north trend. Temperature and salinity were highest at the surface of station
252 M30, due to strong net evaporation in the subtropical gyre (Fig. 2a and b). There was a northward decrease in temperature and
253 salinity due to the influence of upwelling in the subarctic gyre. ~~The surface mixed layer depth, defined as the depth where~~
254 ~~potential density increases by 0.03 kg m^{-3} compared to that at the sea surface, varied around 11–25 m.~~

255 In contrast to temperature and salinity and as expected, the distribution of ~~dissolved inorganic nitrogen (DIN, nitrate plus~~
256 ~~nitrite)~~, SRP and ~~dissolved silicate (DSi)~~ showed a generally northward increasing pattern (Figs. 2c–d and S1a). Surface DIN
257 concentrations were ~~below the detection limit on~~ average $0.006 \mu\text{mol L}^{-1}$ in the NPSG region and averaged $0.02 \mu\text{mol L}^{-1}$ in
258 the Kuroshio-Oyashio transition region. ~~The top of the nutrient line, defined as the depth where DIN concentrations reach 0.1~~
259 ~~$\mu\text{mol L}^{-1}$, ranged from 110 m at station M30 to 20 m at station STN45.~~ The ammonium (NH_4^+) concentration above 100 m at
260 station STN45 was notably higher than that at other stations (Fig. S1b). ~~Similar to the nutrient line distribution, the~~ deep
261 chlorophyll maximum (DCM) depth gradually shoaled northward from 110 m at station M30 in the NPSG region to 33 m at
262 station STN45 in the Kuroshio-Oyashio transition region (Fig. 2e).

263

带格式的: 缩进: 首行缩进: 0 字符



带格式的: 两端对齐

带格式的: 居中

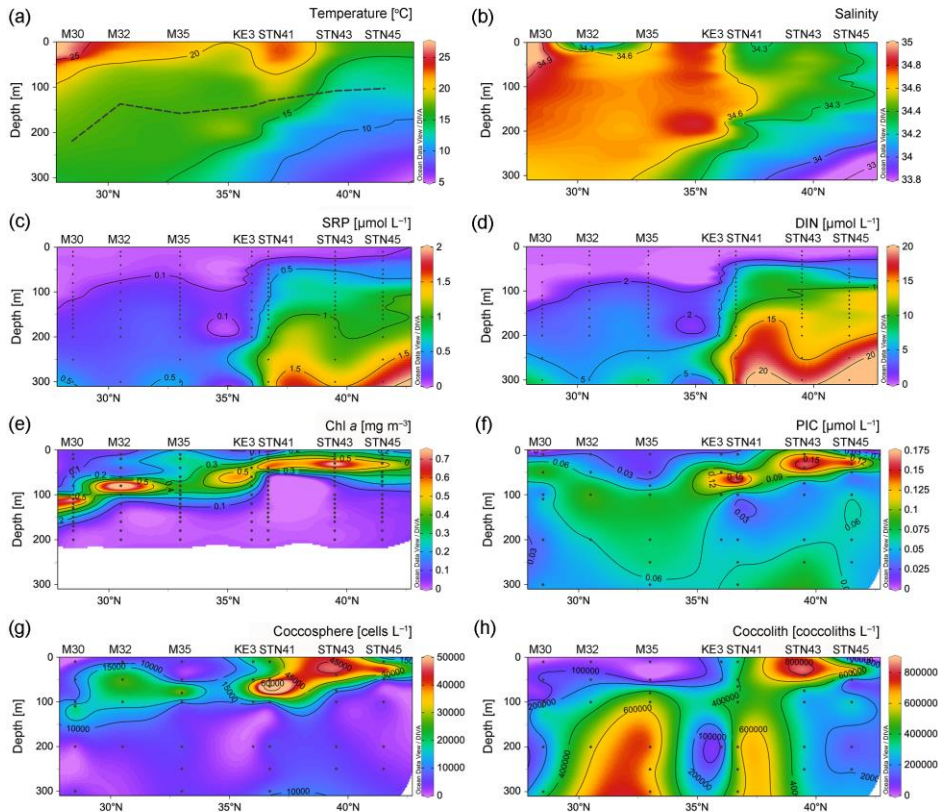


Fig. 2. Vertical depth distributions of (a) temperature, (b) salinity and concentrations of (c) soluble reactive phosphate (SRP), (d) dissolved inorganic nitrogen (DIN, nitrate plus nitrite), (e) Chlorophyll *a* (Chl *a*), (f) particulate inorganic carbon (PIC), (g) coccosphere cell and (h) detached coccoliths in the upper 300 m of the water column in the study area. In (a), the black dashed line indicates the bottom of the euphotic zone.

271 **3.2 Vertical distribution of PIC and coccolithophore concentrations**

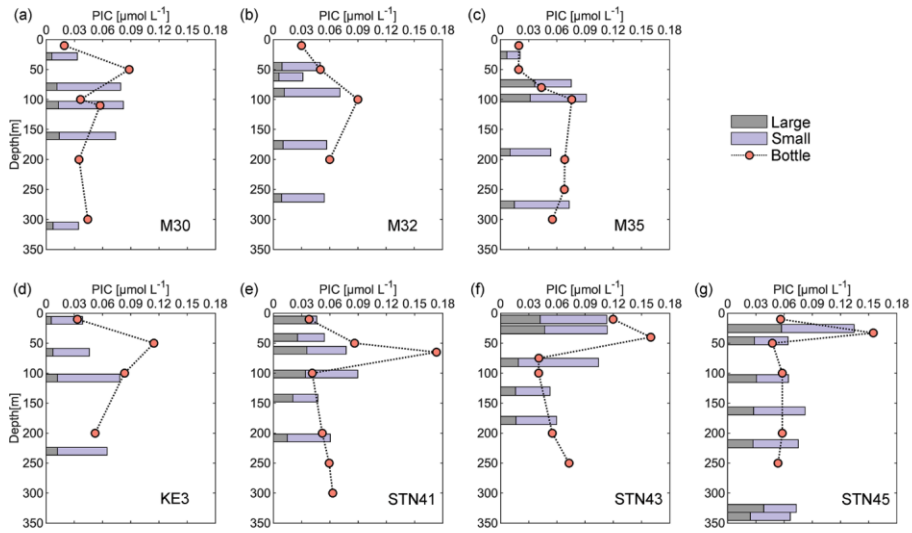
272 PIC concentrations along the 155°E transect ranged from 0.02 to 0.17 $\mu\text{mol L}^{-1}$, with an average of $0.06 \pm 0.04 \mu\text{mol L}^{-1}$ in
273 the upper 300 m of the water column (Fig. 2f). Generally, PIC concentrations were lower at the surface and increased with
274 increasing depth to attain a maximum in the DCM layer, and decreased with depth thereafter. In the DCM layer, PIC
275 concentrations ranged from 0.06 $\mu\text{mol L}^{-1}$ at 110 m of station M30 in the subtropical gyre to 0.16 $\mu\text{mol L}^{-1}$ at 33 m of station
276 STN45 in the Kuroshio-Oyashio transition region. The vertical distribution pattern of bottle-derived PIC and coccosphere cell
277 concentrations overall followed that of Chl *a*, showing a northward shoaling of the subsurface maximum.

278 Concentrations of coccosphere cells ranged from ca. 970 to 75,000 cells L^{-1} (Fig. 2g). Along the transect, a subsurface
279 maximum was evidenced around the DCM layer with an average of 42,000 cells L^{-1} , followed by a steep decrease below 100
280 m. The highest coccosphere cell concentration was observed at 65 m of station STN41, corresponding to the highest PIC
281 concentration. The average coccosphere cell concentration was notably lower in the NPSG region (9,800 cells L^{-1}) than in the
282 transition region (18,000 cells L^{-1}). The detached coccolith concentration averaged 340,000 coccoliths L^{-1} , with a range of
283 11,000 to 800,000 coccoliths L^{-1} (Fig. 2h). The highest concentration was observed around 10–40 m of station STN43. High
284 coccolith concentrations were also observed below 100 m at stations M32, M35 and STN41.

285 Size-fractionated PIC concentrations from in situ pumps varied from 0.01 to 0.09 $\mu\text{mol L}^{-1}$ in the SSF-small size fraction
286 and from 0.01 to 0.06 $\mu\text{mol L}^{-1}$ in the large size fraction. LSF-PIC concentrations averaged $0.07 \pm 0.02 \mu\text{mol L}^{-1}$,
287 and were comparable to bottle-derived PIC concentrations (Fig. 3). Roughly 70 % of the PIC was contributed by the small size
288 fraction. SSF at each sampling station. Generally, large size fraction PIC concentrations increased northward from
289 stations M30–M35 to stations KE3–STN45 and accounted for 22 % and 36 % of total PIC concentrations in the NPSG
290 region and the Kuroshio-Oyashio transition region, respectively. The maximum concentration of large size-fractionated PIC
291 LSF-PIC (0.06 $\mu\text{mol L}^{-1}$) was observed at 26 m of station STN45 (Fig. 3g).

292

带格式的: 缩进: 首行缩进: 0 字符



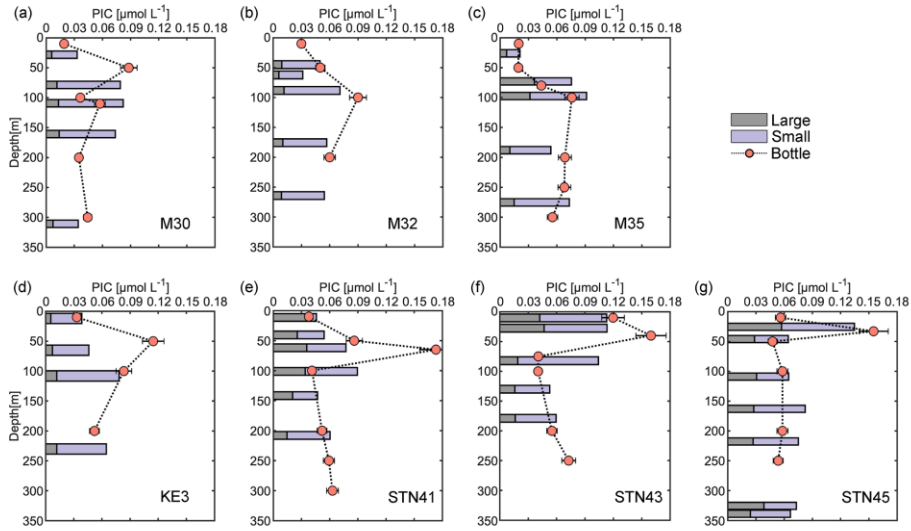


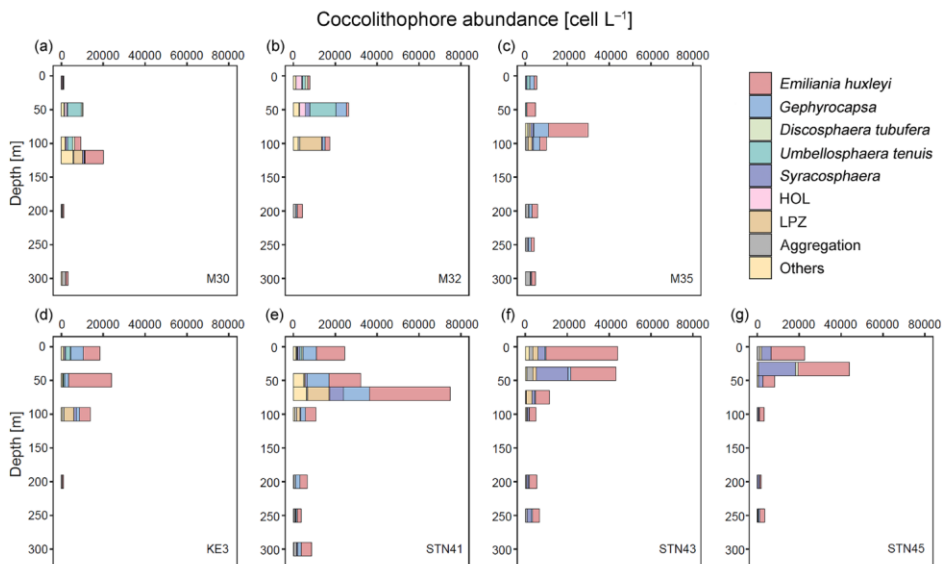
Fig. 3. Vertical depth distributions of particulate inorganic carbon (PIC) concentrations derived from sampling using both Niskin bottles and in situ pumps (small size fraction of 1–51 μm and large size fraction of $> 51 \mu\text{m}$) in the upper 350 m of the water column at sampling stations in the study area.

3.3 Characteristics of the coccolithophore assemblage

Coccolithophore populations were predominantly represented by *Emiliania huxleyi*, *Gephyrocapsa ericsonii*, *Gephyrocapsa oceanica*, *Umbellosphaera tenuis*, *Syracosphaera* spp., holo-coccolithophores (HOL), *Algirosphaera robusta*, and *Florisphaera profunda* (each comprising $> 1\%$ of total coccosphere abundance; Fig. 4). In surface water, coccolithophore cells were dominated by *Dicosphaera tubifera*, *U. tenuis* and HOL at stations M30 and M32 (Fig. 4a and b) and by *G. ericsonii* at stations M35, KE3 and STN41 (Fig. 4c, d and e), while high abundance of *E. huxleyi* and *Syracosphaera* spp. was clearly observed at stations STN43 and STN45 (Fig. 4f and g). It is noteworthy that *E. huxleyi* contributed the largest fraction (50 %) to the total coccolithophore assemblage-cells and was also found to be the dominant species in the DCM layer. *U. tenuis* was

307 mainly observed in subtropical gyre waters, with peak abundance at 50 m and lower abundance at the surface and in the DCM
 308 waters (Fig. 4a and b). Lower euphotic zone (LPZ, defined as the region of the water column that receives 10–1% of surface
 309 PAR) coccolithophore species (including *A. robusta* and *F. profunda*) were commonly found in the subsurface population
 310 below 50 m, accounting for 7 % of the entire coccolithophore community (Jin et al., 2016; Poulton et al., 2017). Overall,
 311 coccolithophores were scarce in the NPSG region and dominated by *U. tenuis*, whereas their abundance notably increased in
 312 the Kuroshio-Oyashio transition region where it was dominated by *E. huxleyi*, *Gephyrocapsa* and *Syracosphaera* spp..

313



314

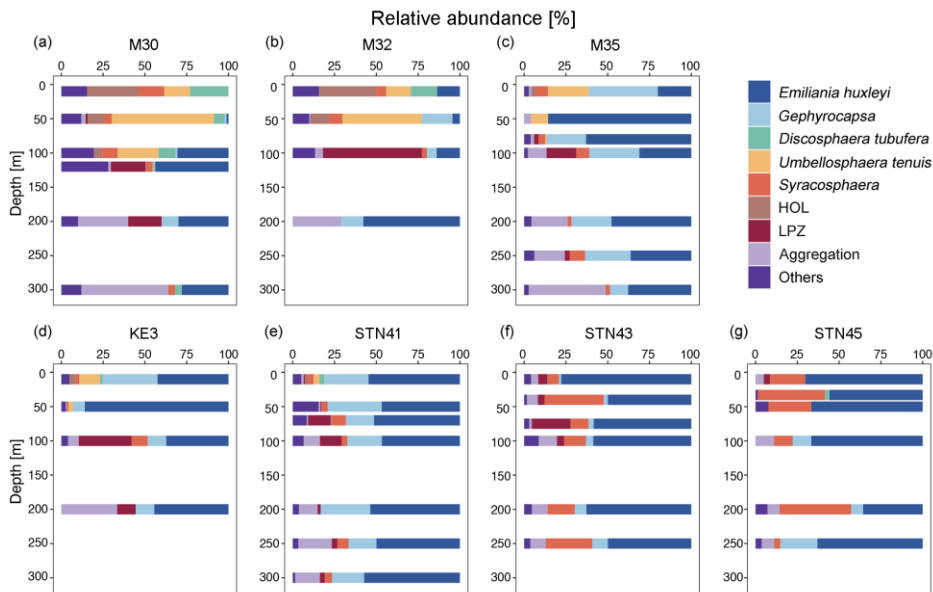
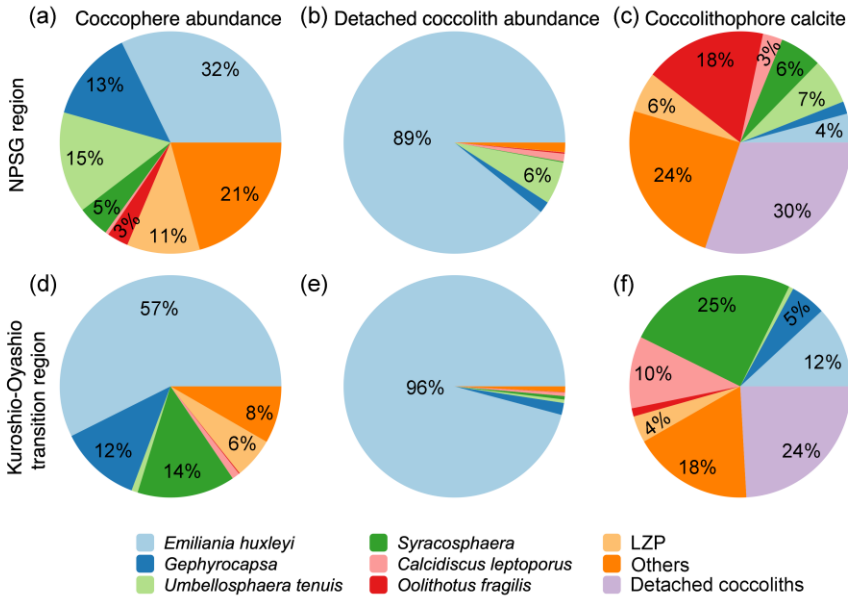


Fig. 4. Relative Abundance of different coccolithophore groups in the upper 300 m of the water column **at sampling stations in the study area**. Lower euphotic zone (LPZ) species include *Florisphaera profunda* and *Algirosphaera robusta*; HOL indicates holo-coccolithophores.

The estimated coccolithophore calcite concentrations ranged from <0.010 to $0.23 \mu\text{mol L}^{-1}$, averaging $0.05 \pm 0.04 \mu\text{mol L}^{-1}$ above 300 m along the 155°E transect. The coccospheres of *E. huxleyi* accounted for 50–32 % and 57 % of the total coccolithophore assemblage-cells but represented only 9–4 % and 12 % of the coccolithophore calcite concentration in the NPSG region and the Kuroshio-Oyashio transition region, respectively (Fig. 5a and e). In the NPSG region, *U. tenuis* accounted for 15 % of the total coccolithophore cells and 7 % of the coccolithophore calcite concentration, both notably higher than in the transition region, where its contribution was <1 % for both measures. The less abundant (<1 %) species *Calcidiscus leptoporus* and *Oolithotus fragilis* accounted for 7.5 % and 7.7 % of the coccolithophore calcite concentration, respectively.

327 *Syracosphaera* spp. was the largest contributor in the Kuroshio-Oyashio transition region, accounting for 47.725 % of the
 328 coccolithophore calcite concentration (Fig. 5ef). The less abundant (<3 %) species *Calcidiscus leptoporus* and *Oolithotus*
 329 *fragilis* accounted for 21 % and 12 % of the coccolithophore calcite concentration in the NPSG region and the Kuroshio-
 330 *Oyashio transition region, respectively.* Additionally, *E. huxleyi*-detached coccoliths comprising 94 % of the total detached
 331 coccoliths, made up contributed to ~16 %30 % and 24 % of the total coccolithophore calcite concentration in the two regions,
 332 respectively (Fig. 5b-5c and ef).

333



334

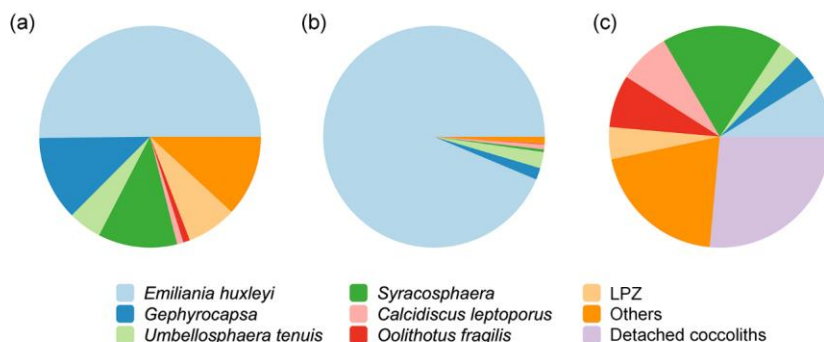


Fig. 5. Contribution of different coccolithophore groups to coccosphere cell abundance, detached coccolith abundance, and coccolithophore calcite concentrations in the upper 300 m of the water column in (a–c) the North Pacific Subtropical Gyre (NPSG, stations M30, M32 and M35) and (d–f) the Kuroshio-Oyashio transition region (stations KE3, STN41, STN43 and STN45). **Fig. 5.** Contribution of different coccolithophore groups to (a) coccosphere cell abundance, (b) detached coccolith abundance and (c) coccolithophore calcite concentration in the upper 300 m of the water column. Lower euphotic zone (LPZ) species include *Florisphaera profunda* and *Algirosphaera robusta*.

3.4 CaCO₃ standing stock and production

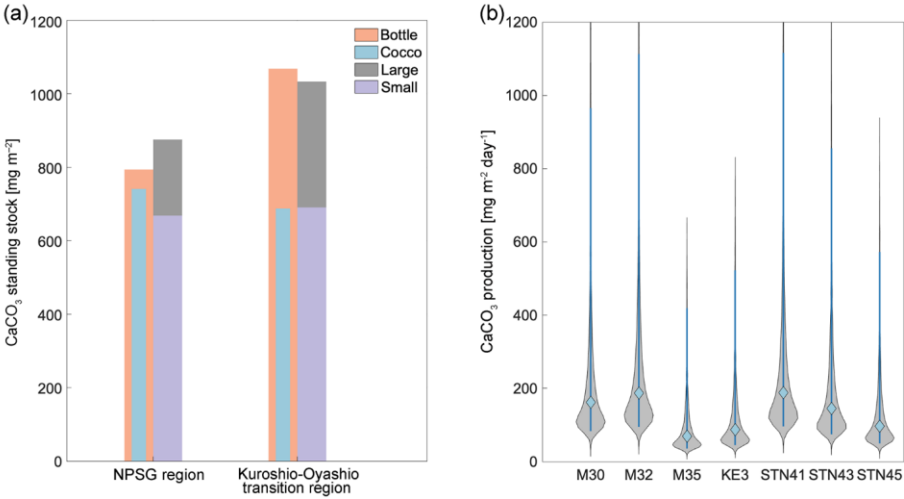
The standing stocks of CaCO₃ in the euphotic zone were determined using data from Niskin bottles, coccolithophore calcite, and size-fractionated samples (Fig. 6a). The standing stock of CaCO₃ was determined by considering the first shallow sampling depth to a consistent depth of 150 m (Figs. 6a and S2a). CaCO₃ standing stock derived from Niskin bottle-sampling ranged from 660–7.0 to 1,200–11.1 mmol m⁻² mg m⁻², and was slightly lower in the oligotrophic NPSG region (790–8.7 ± 1.7 mmol m⁻² mg m⁻²) than in the relatively nutrient-high Kuroshio-Oyashio transition region (9.2 ± 1.7 mmol m⁻² 1,100 mg m⁻²). Based on the estimated coccolithophore calcite concentrations, CaCO₃ standing stocks ranged from 370 to 1,000 mg m⁻² 4.0 to 11.3 mmol m⁻² and peaked at station STN41/M30 due to its deepest euphotic zone (Fig. 2a and 6a). Calcite from coccolithophores comprised on average 76–979 ± 27 % of the CaCO₃ standing stock from Niskin bottle samples, and the contribution was

带格式的: 非上标/下标

352 higher in the NPSG region ($91 \pm 30\%$) than in the Kuroshio-Oyashio transition region ($65\text{--}70 \pm 24\%$); Fig. 6b)(Fig. 6a),
353 demonstrating the vital role of coccolithophores in CaCO_3 production, particularly in oligotrophic ocean waters.

354

355



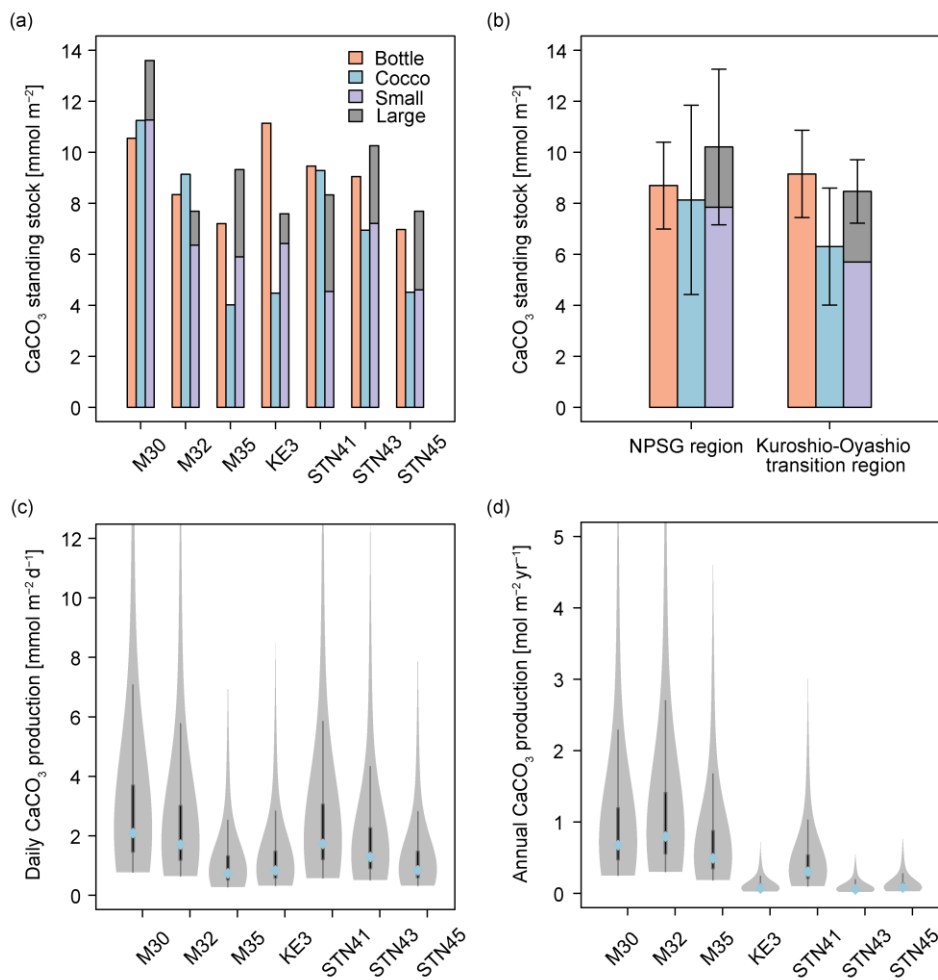


Fig. 6. Calcium carbonate (CaCO₃) standing stock in the euphotic zone estimated from Niskin bottle particulate inorganic carbon (PIC), total calcite (Cocco) and size-fractionated (large and small fractions indicate > 51 and 1–51 μm, respectively) PIC concentrations (a) at each sampling station and (b) in the North Pacific Subtropical Gyre (NPSG) and Kuroshio-Oyashio

transition regions; (c) CaCO_3 production by coccolithophores in the euphotic zone at indicated sampling stations in June–July 2022; (d) annual CaCO_3 production corrected for seasonal bias using satellite-derived PIC concentrations. In (c) and (d), the blue diamond marks the median value, while the shaded area displays the probability density of the estimates. The grey lines denote the 25% and 75% quartiles.

Fig. 6. (a) Calcium carbonate (CaCO_3) standing stock in the upper 150 m water column estimated from Niskin bottle particulate inorganic carbon (PIC), total calcite (Cocceo) and size-fractionated (large and small fractions indicate > 51 and $1–51 \mu\text{m}$, respectively) PIC concentrations in the North Pacific Subtropical Gyre (NPSG) and Kuroshio–Oyashio transition regions; (b) CaCO_3 production by coccolithophores in the upper 150 m water column at indicated sampling stations in June–July 2022.

Total CaCO_3 standing stock derived from in situ pump samples ranged from 7.6 to 13.6 mmol m^{-2} to $1,300 \text{ mg m}^{-2}$, averaging $10.2 \pm 3.1 \text{ mmol m}^{-2}$ to 880 mg m^{-2} in the subtropical gyre and $8.5 \pm 1.2 \text{ mmol m}^{-2}$ to $1,030 \text{ mg m}^{-2}$ in the transition region, consistent with results from Niskin bottle samples. The CaCO_3 standing stock of the SSF-small PIC ranged from 4.5 to 11.3 mmol m^{-2} to 514 to 904 mg m^{-2} and accounted for $71 \pm 12\%$ to 71% of the total standing stock in the entire research domain (Fig. 6a).

Given that coccolithophores have a turnover time of 0.7–10 days (Krumhardt et al., 2017; Ziveri et al., 2023), CaCO_3 production rate in the upper 150 m of the water column euphotic zone ranged from 70 to $190 \text{ mg m}^{-2} \text{ d}^{-1}$ to 0.8 to $2.1 \text{ mmol m}^{-2} \text{ d}^{-1}$ during the sampling period (Fig. 6b,c). Generally, the coccolithophore CaCO_3 production was comparable in the subtropical gyre and the Kuroshio–Oyashio transition region, averaging 1.5 ± 0.7 to 140 ± 62 and $1.2 \pm 0.4 \text{ mmol m}^{-2} \text{ d}^{-1}$ to $130 \pm 46 \text{ mg m}^{-2} \text{ d}^{-1}$, respectively. Coccolithophore CaCO_3 production in the euphotic zone was maximal at station STN41–M30 where it reached $190 \text{ mg m}^{-2} \text{ d}^{-1}$, corresponding to the maximum coccosphere cell concentration (Fig. 2e). and The the lowest coccolithophore CaCO_3 production of $70 \text{ mg m}^{-2} \text{ d}^{-1}$ was observed at station M35 in the NPSG region.

4 Discussion

4.1 Contribution of coccolithophore calcite to PIC

In this study, bottle- and pump-derived PIC concentrations generally agreed with each other (Fig. 3), and both were on the

385 same order of magnitude as suspended PIC concentrations measured in the Atlantic, Indian and Pacific Oceans (Beaufort et
386 al., 2008; Barrett et al., 2014; Lam et al., 2015, 2018; Maranón et al., 2016). Coccolithophore calcite concentrations showed a
387 significant positive correlation with PIC concentrations ($r^2 = 0.52$, $p < 0.01$, $n = 40$; Fig. 7a), highlighting the major contribution
388 of coccospheres and detached coccoliths (68 %) to total CaCO_3 in the upper 300 m of the water column. This is consistent
389 with findings from the eastern North Pacific Ocean where coccolithophores dominate CaCO_3 production (Ziveri et al., 2023).
390 It is noteworthy that detached coccolith concentrations of *E. huxleyi*, *U. tenuis* and *Syracosphaera* spp. showed a significant
391 positive relationship with their coccosphere cell concentrations (Fig. 7b–d), indicating that those detached particles were likely
392 shed by cells as part of the dynamic calcification process, during which coccoliths are continuously produced and released
393 (Johns et al., 2023). However, other potential sources and processes, such as advection, cell disintegration from viral lysis and
394 grazing, fecal pellets, or the dissolution associated with microbial respiration could also contribute to the observed detached
395 coccolith concentrations (Subhas et al., 2022; Vincent et al., 2023; Dean et al., 2024). Coccolith production and shedding vary
396 among species. Fast-growing species like *E. huxleyi* produce and shed coccoliths rapidly during exponential growth phases,
397 whereas other species exhibit different patterns, which are influenced by their distinct physiological and ecological
398 characteristics (Johns et al., 2023).

带格式的: 非上标/ 下标

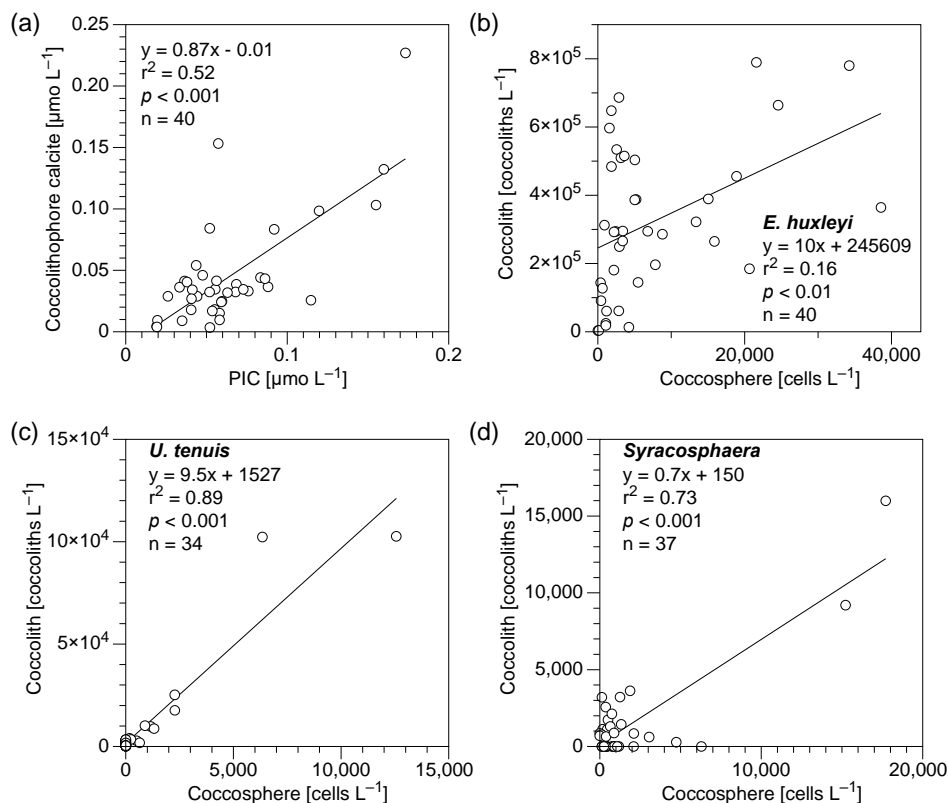


Fig. 7. Relationship of (a) coccolithophore calcite (coccospheres and detached coccoliths) vs particulate inorganic carbon (PIC) concentrations and (b–d) detached coccolith vs coccosphere cell concentrations for (b) *Emiliania huxleyi*, (c) *Umbellosphaera tenuis* and (d) *Syracosphaera* spp. in the upper 300 m water column in the study area. Equations describing the fitted straight lines are also shown.

The less abundant (<3 %) species such as *C. leptoporus* and *O. fragilis* also made a large contribution to calcite concentrations, accounting for 21 % and 12 % of the coccolithophore calcite concentration in the NPSG region and the

Kuroshio-Oyashio transition region, respectively (Fig. 5). It has been reported that despite the relatively low numeric abundance (<2 %), some larger species of the coccolithophore community such as *C. leptoporus*, *Helicosphaera carteri* and *Coccolithus pelagicus* may account for most of the coccolithophore CaCO_3 flux to the deep ocean (Rigual Hernández et al., 2020). Some rare coccolithophore species with high coccolith and coccosphere cell concentrations have also been identified as important contributors to both upper-ocean calcite production (Daniels et al., 2016) and deep-sea calcite fluxes (Ziveri et al., 2007). Thus, larger and less abundant coccolithophore species can play an important role in CaCO_3 production and export.

Higher CaCO_3 standing stock in the euphotic zone of the Kuroshio-Oyashio transition region (Fig. 6a) is consistent with satellite observations suggesting that higher surface PIC concentrations occur at high latitudes (Balch et al., 2005; Berelson et al., 2007). In the present study, however, the relative contribution of coccolithophores to the CaCO_3 standing stock was higher in the NPSG region (~91 %) than in the Kuroshio-Oyashio transition region (~70 %) (Fig. 6a). To date, most studies estimated CaCO_3 standing stocks using satellite-derived data, which might be challenging to use in subtropical gyres where the DCM depth usually lies below 100 m (Cornec et al., 2021). In these oligotrophic oceans with low productivity, a subsurface PIC maximum can develop within the euphotic zone, and the highly variable subsurface PIC concentrations are poorly reflected by satellites, potentially limiting the ability to fully capture coccolithophore contributions.

In oligotrophic ocean gyres, subsurface CaCO_3 production could still occur even if surface PIC is low (Balch et al., 2018). Along our studied transect, maximum coccolithophore abundances increased about twofold from the subtropical gyre to the transition region (Fig. 2g), while a much smaller difference was found in the integrated coccolithophore CaCO_3 between the two regions (Fig. 6a). This suggests that subsurface coccolithophore CaCO_3 contributed substantially to the total upper water column PIC concentration in the NPSG region. Coccolithophore groups were diverse in the subtropical gyre, including some rare but relatively large and heavily calcified species that contribute significantly to CaCO_3 production. In the Southern Ocean, coccolithophores contribution to the annual CaCO_3 export is highest in waters with low algal biomass accumulations (Rigual Hernández et al., 2020). Given that low surface PIC regions (<0.1 mmol m^{-3}) occupy about 87 % of the global ocean surface (Ziveri et al., 2023), our data highlight the notable contribution of these regions to global coccolithophore CaCO_3 production.

Size-fractionated PIC concentrations showed a smaller contribution of coccolithophores to the CaCO_3 standing stock in the Kuroshio-Oyashio transition region (67 ± 13 %) than in the NPSG region (76 ± 11 %) (Fig. 6b). This pattern is consistent with

that observed in the eastern North Pacific Ocean (Fig. 8), which suggests that the contribution of small PIC to CaCO_3 standing stock is lower in the subpolar gyre (65 %) than in the subtropical gyre (84 %). In other words, the contribution of large size fraction PIC (e.g., zooplanktonic foraminifera, pteropods and heteropods) to CaCO_3 standing stock is higher in the subpolar gyre (35 %) than in the subtropical gyre (16 %) of the eastern North Pacific Ocean (Ziveri et al., 2023). Betzer et al. (1984) reported that foraminifera calcite is more abundant in northern regions (north of 42°N) of the western North Pacific. At Ocean Station Papa in the northeast Pacific (50°N , 145°W), model results showed that foraminifera calcite accounts for only 18–30 % of the total CaCO_3 production, whereas coccolithophores are the main producer, contributing to 59–77 % of the total CaCO_3 production (Fabry, 1989). These findings support our results and suggest that the relatively high contribution of large size fraction PIC in the northern region of the western North Pacific is likely attributed to foraminifera.

In the Atlantic Ocean, coccolithophore calcite fluxes and species richness are higher in subtropical than in temperate waters, which is ascribed to the reduced competition with diatoms in the former (Broerse et al., 2000). Note that a clear latitudinal gradient of diatom biomass was observed along 160°E in the North Pacific Ocean, consistent with findings from phytoplankton pigment analysis and ocean-color satellite observations (Hirata et al., 2011; Sugie and Suzuki, 2017). The distribution of planktic foraminifera in the North Pacific has been linked to phytoplankton productivity and food availability, with higher abundance in the transitional region compared to the subtropical region (Taylor et al., 2018). Based on these findings, we suggest that differences in ecosystem structure among sites modulate the relative contribution of various calcifiers to pelagic PIC production. The higher abundance of non-calcareous phytoplankton (e.g., diatoms) in the transition zone could also reduce coccolithophore biomass via resource competition (Quere et al., 2005; Sinha et al., 2010) and stimulate the growth of foraminifera (Schiebel et al., 2017), resulting in the observed decreased contribution of small coccolithophores to total CaCO_3 production. Sediment trap data from the North Pacific also support this pattern, indicating lower fluxes of planktonic foraminifera, organic matter, and biogenic opal in the subtropical region but elevated fluxes in the transitional and subarctic regions (Eguchi et al., 2003).

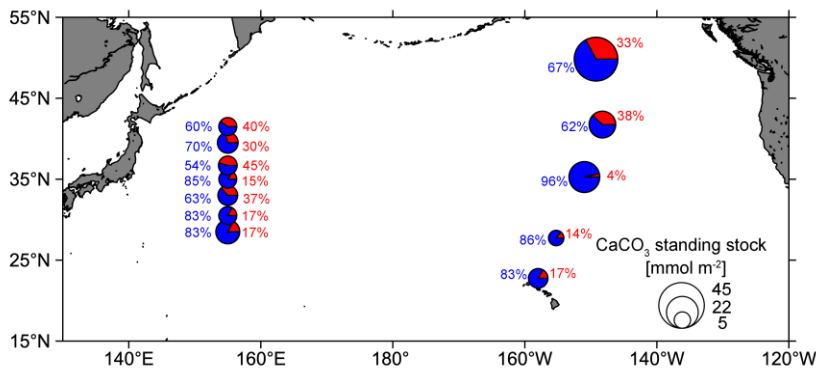


Fig. 8. Pie charts showing the composition of the total calcium carbonate (CaCO_3) standing stock in the euphotic zone of the western (this study) and eastern North Pacific Ocean (data from the CDisK-IV cruise; Ziveri et al., 2023). Red represents the standing stock of large size-fractionated ($> 51 \mu\text{m}$) CaCO_3 from this study, and planktonic foraminifera, pteropods and heteropods from the CDisK-IV cruise. Blue represents the standing stock of small size-fractionated ($1\text{--}51 \mu\text{m}$) CaCO_3 from this study and coccolithophores from the CDisK-IV cruise.

4.14.2 Coccolithophore responses to environmental factors

Coccolithophores are an important component of phytoplankton biomass and fill a variety of ecological niches in global oceans. They inhabit different marine environments from oligotrophic to eutrophic, warm to cold, euphotic to aphotic, and stratified to mixed (Balch, 2018). It is of critical importance to evaluate the response of coccolithophore species to different environmental conditions to better understand changes in coccolithophore species diversity, community composition, and their role in the oceanic carbon cycle.

Although biogeographical zones of coccolithophores in the North and Central Pacific were identified a couple of decades ago, few studies have investigated coccolithophore distributions in the North Pacific over the recent two decades (Okada and Honjo, 1973; Hagino et al., 2005). In the western North Pacific Ocean, higher diversity and less abundant coccolithophore assemblages were observed in the oligotrophic subtropical gyres, whereas the Kuroshio-Oyashio transition region tended to exhibit a lower

带格式的: 缩进: 首行缩进: 0 字符

diversity corresponding to higher PIC and coccolithophore concentrations (Figs. 2 and S3S2). This finding is consistent with results from the Atlantic Ocean, and a result of the different survival strategies of various coccolithophore species (Poulton et al., 2017; Balch et al., 2019). Coccolithophores are nutrient stress tolerant and have lower iron cell quotas, and are thus generally abundant in the open ocean (Gregg and Casey, 2007; Brun et al., 2015). Prior studies have shown that coccolithophores, particularly *E. huxleyi*, can grow more effectively under low iron conditions than other phytoplankton such as diatoms (Hartnett et al., 2012; Balch, 2018). However, when nutrients and light are plentiful, the heavy coccoliths of this group of phytoplankters pose a selective disadvantage over diatoms and chlorophytes (Gregg and Casey, 2007). The dominance of coccolithophores in the Great Calcite Belt is primarily driven by their adaptation to low iron levels, which, together with low surface DSi concentrations, limit diatom growth (Balch et al., 2016). The majority of coccolithophore species are K-selected, characterized by relatively slow-growth, large cell size and are more competitive in low-nutrient and well-stratified regions (Brand, 1994), whereas only few r-selected species (such as the fast-growing and small-sized *E. huxleyi*) mainly survive thrive in relatively dynamic and nutrient-rich regions (Charalampopoulou, 2011; Brun et al., 2015; O'Brien et al., 2016). In the present study, the most abundant and widely distributed coccolithophore species was *E. huxleyi*, which showed increasing abundance northward along the study transect (Fig. 4). This is consistent with prior observations demonstrating that *E. huxleyi* is the most abundant coccolithophore species in the subarctic, subantarctic and bordering transitional regions (Saavedra-Pellitero et al., 2014).

According to the RDA results, environmental variables accounted for 47.6 % of the total variation in coccolithophore community composition (Fig. 7a9a). The first two RDA axes suggested that there were significant spatial differences in the coccolithophore community across depths and regions (Fig. S43). In the tropical and subtropical Atlantic Ocean, coccolithophore communities exhibit greater variability vertically within the water column than horizontally, at spatial scales of hundreds to thousands of kilometers (Poulton et al., 2017). Moreover, distinct species distributions are identified based on the depth zones (upper euphotic, lower euphotic, and subeuphotic zones), which reflect the lifestyle of the species (Poulton et al., 2017; Balch, 2018). In the NPSG region, our results also reveal a distinct vertical distribution pattern (Fig. 4), which may have been driven by factors such as light availability, temperature, and nutrient levels. These environmental variables likely contribute to the physiological diversity of coccolithophores. A shift in dominant species occurred from *U. tenuis* and *E. huxleyi*

498 in the NPSG region to *Syracosphaera* spp. and *E. huxleyi* in the transition region (Fig. 5). This is consistent with the prior
499 observations of Balch et al. (2019). Correspondingly, hierarchical partitioning analysis showed that depth and latitude had a
500 significant effect on coccolithophore community variation ($p < 0.05$). Other environmental factors, such as temperature,
501 salinity, Chl *a* and TA ~~were also important influencing-influenced~~ the coccolithophore community (Fig. 7b9b).

502 Based on Spearman's correlation analysis, coccolithophore abundance showed a significant positive relationship with
503 temperature, Ω_{calcite} and pH, and a significant negative relationship with depth, DIC and macro-nutrient concentrations,
504 especially for *D. tubifera*, *U. tenuis* and *HOL* that are more sensitive to environmental factors (Fig. 7e9c). The positive
505 correlation with temperature is consistent with field observations and model simulations pointing to a general trend of
506 increasing coccolithophore abundance in the context of global warming (Rivero-Calle et al., 2015; Rousseaux and Gregg,
507 2015). More abundant species like *E. huxleyi* and *Syracosphaera* spp., however, only showed a highly positive correlation
508 with depth, latitude and Chl *a* concentration, suggesting that these species are more adaptable to varying environmental
509 conditions (Schlüter et al., 2014). ~~Using random forest analysis, we also determined that the best predictors of coccolithophore~~
510 ~~abundance were Chl *a* concentration, depth and Ω_{calcite} ($p < 0.01$; Fig. 7d).~~ In the Atlantic Ocean, *E. huxleyi* has been observed
511 to exhibit an increasing relative abundance with increasing latitude (Balch et al., 2019; Holligan et al., 2010; Poulton et al.,
512 2017). Unlike many other species, *E. huxleyi* has a widespread distribution attributed to its ability to adapt to diverse
513 environments through both phenotypic plasticity and genetic selection (Lohbeck et al., 2012; Rickaby et al., 2016b; Taylor et
514 al., 2017). Our results indicate that less abundant species, such as *C. leptoporus* and *O. fragilis*, also contributed to
515 coccolithophore calcite concentrations (Fig. 5). Their calcification is species-specific, predominantly driven by inherent
516 biological traits, including cell shapes, coccolith types, and architectural variations, which are conservative features of
517 coccolithophore biology (Rickaby et al., 2016a). However, the weak correlation of *C. leptoporus* and *O. fragilis* with
518 environmental factors might be due to their low abundance. Overall, our study highlights the significant influence of depths
519 and latitude on coccolithophore community composition, emphasizing the complex interplay between biotic and abiotic factors.

520

带格式的: 缩进: 首行缩进: 0 字符

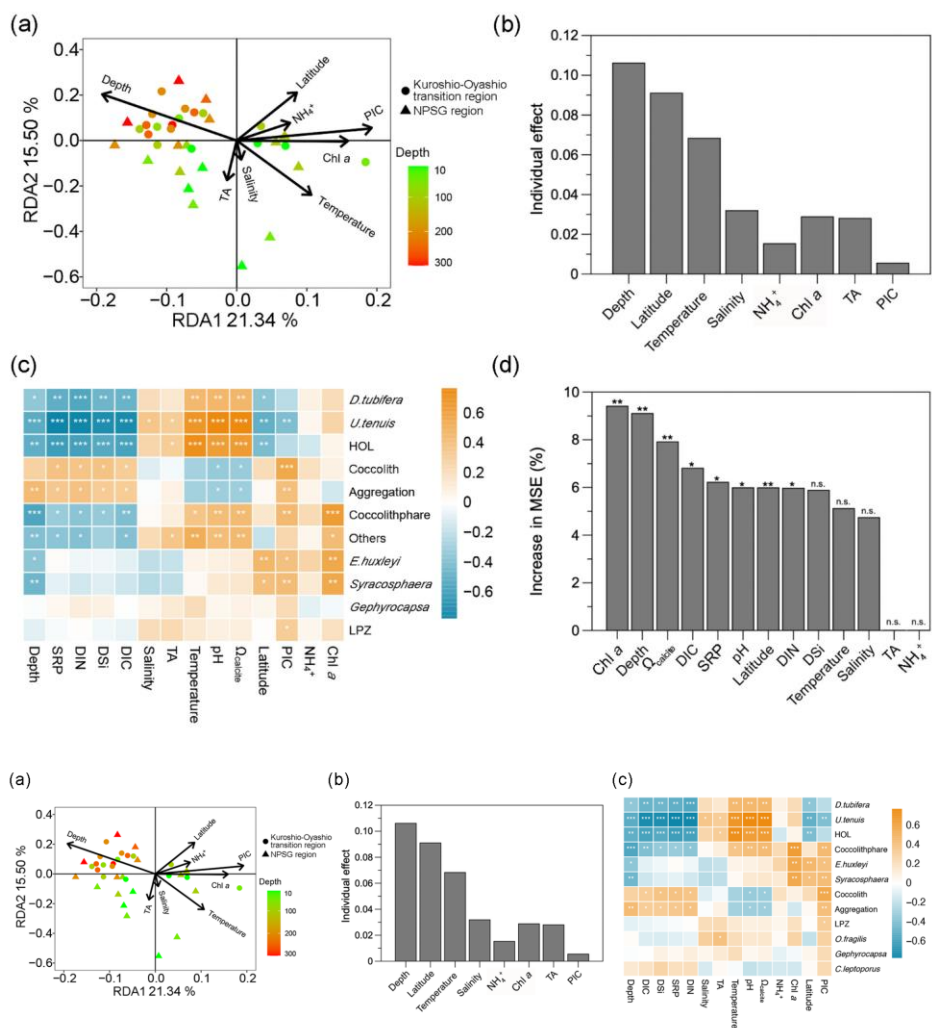


Fig. 79. (a) Redundancy analysis (RDA) diagram illustrating the relationship between the coccolithophore community and

environmental factors; (b) independent contribution of each environmental factor to coccolithophore community variation using hierarchical partitioning-based canonical analysis; (c) correlations between coccolithophore groups and environmental factors with color gradients denoting the significance of the Spearman's correlation coefficient r . Asterisks represent the statistical significance ($***p < 0.001$, $**p < 0.01$, $*p < 0.05$); (d) random forest mean predictor importance, i.e., the percentage of increase in the mean variance error (MSE) of environmental factors on coccolithophore abundance ($**p < 0.01$, $*p < 0.05$, n.s., non-significant). Chl a : chlorophyll a , DIC: dissolved inorganic carbon, TA: total alkalinity, Ω_{calcite} : saturation state with respect to calcite, PIC: particulate inorganic carbon, DIN: dissolved inorganic nitrogen (nitrate plus nitrite), NH_4^+ : ammonium, SRP: soluble reactive phosphate, DSi: dissolved silicate, HOL: holo-coccolithophores and LPZ: lower euphotic zone species *Florisphaera profunda* and *Algirosphaera robusta*.

4.2 Contribution of coccolithophore calcite to PIC

In this study, bottle- and pump-derived PIC concentrations generally agreed with each other (Fig. 3), and both were comparable to and of the same order of magnitude as the suspended PIC concentrations detected in the Atlantic, Indian and Pacific Oceans (Beaufort et al., 2008; Barrett et al., 2014; Lam et al., 2015, 2018; Marañón et al., 2016). Coccolithophore calcite concentrations showed a significant positive correlation with PIC concentrations ($r^2 = 0.75$, $p < 0.01$, $n = 40$; Fig. 8a), highlighting the major contribution of coccospheres and detached coccoliths (68 %) to the total CaCO_3 in the upper 300 m of the water column. This is consistent with findings from the eastern North Pacific Ocean where coccolithophores dominate CaCO_3 production (Ziveri et al., 2023). It is noteworthy that detached coccolith concentrations of *E. huxleyi*, *U. tenuis* and *Syracosphaera* spp. showed a significant positive relationship with their coccosphere cell concentrations (Fig. 8b-d), indicating that those detached particles were likely to have originated from living cells.

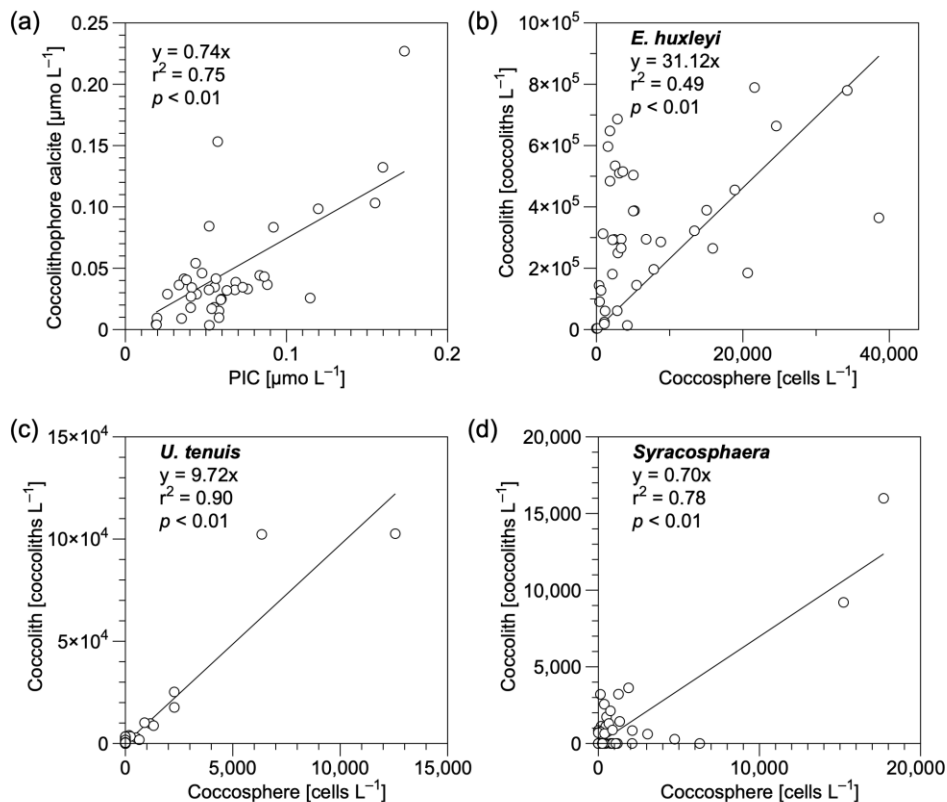


Fig. 8. Relationship of (a) coccolithophore calcite vs particulate inorganic carbon (PIC) concentrations and (b–d) detached coccolith vs coccosphere cell concentrations for (b) *Emiliania huxleyi*, (c) *Umbellosphaera tenuis* and (d) *Syracosphaera* spp. in the upper 300 m water column at the study site. Equations describing the fitted straight lines are also shown.

Abundant coccolithophore groups, including *E. huxleyi*, *Syracosphaera* spp., LPZ species and aggregation, showed a significant positive relationship with PIC concentration (Fig. 7e), but less abundant species like *C. leptopus* and *O. fragilis* also made a large contribution to calcite concentrations. It has been reported that despite the relatively low abundance (< 2 %)

of the coccolithophore community, some larger species such as *C. leptoporus*, *Helicosphaera carteri* and *Coccolithus pelagicus* could account for most of the coccolithophore CaCO_3 flux to the deep ocean (Rigual Hernández et al., 2020). Some rare coccolithophore species with high coccolith and coccosphere cell concentrations have also been identified as important contributors to both upper ocean calcite production (Daniels et al., 2016) and deep sea calcite fluxes (Ziveri et al., 2007). Thus, although *E. huxleyi* is one of the most abundant species in the ocean, larger coccolithophore species can also play an important role in CaCO_3 export.

Higher CaCO_3 standing stock in the upper 150 m of the Kuroshio-Oyashio transition region (Fig. 6a) is consistent with satellite observations suggesting that higher surface PIC concentrations occur at high latitudes (Baleh et al., 2005; Berelson et al., 2007). In the present study, however, the relative contribution of coccolithophores to the CaCO_3 standing stock was higher in the NPSG region (~91 %) than in the Kuroshio-Oyashio transition region (~65 %) (Fig. 6a). To date, most studies estimated CaCO_3 standing stock using satellite-derived data, which might be challenging to use in subtropical gyres where the DCM depth usually lies below 100 m. Because coccolithophore CaCO_3 is largely produced in the lower layer of the euphotic zone and is thus difficult to detect by satellites, coccolithophore contributions could be underestimated.

In oligotrophic ocean gyres, subsurface CaCO_3 production could still occur even if surface PIC is low (Baleh et al., 2018). Along our studied transect, maximum coccolithophore abundances increased about twofold from the subtropical gyre to the transition region (Fig. 2c), while a much smaller difference was found in the integrated coccolithophore CaCO_3 between the two regions (Fig. 6a). This suggests that subsurface coccolithophore CaCO_3 contributed substantially to the total upper water column PIC flux in the NPSG. Coccolithophore groups were diverse in the subtropical gyre, where the environmental conditions favor slow growing, large and heavy species, which account for a large fraction of CaCO_3 production. In the Southern Ocean, coccolithophores contribute to the highest annual CaCO_3 export in waters with low algal biomass accumulations (Rigual Hernández et al., 2020). Given that low surface PIC regions ($< 0.1 \text{ mmol m}^{-3}$) occupy ~87 % of the global ocean surface (Ziveri et al., 2023), our data suggest that coccolithophore CaCO_3 production in subsurface waters constitutes an important part of global pelagic CaCO_3 production.

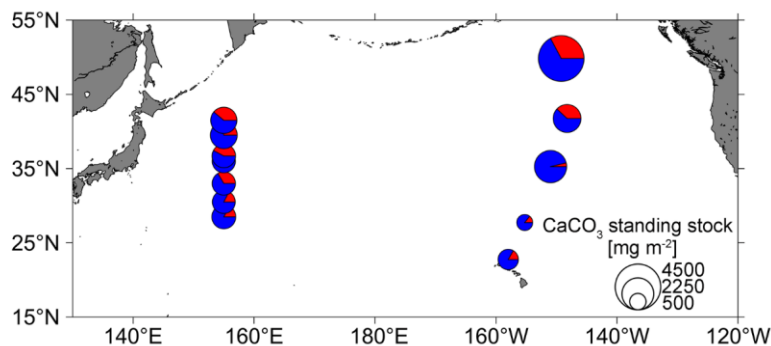
Size-fractionated PIC concentrations showed a smaller contribution of coccolithophores to the CaCO_3 standing stock in the Kuroshio-Oyashio transition region (67 %) than in the NPSG region (76 %) (Fig. 6a), consistent with observations from the

577 eastern North Pacific Ocean (Fig. 9). The contribution of LSF PIC (e.g., zooplanktonic foraminifera, pteropods and heteropods)
 578 to CaCO_3 standing stock is higher in the subpolar gyre (35 %) than in the subtropical gyre (16 %) of the eastern North Pacific
 579 Ocean (Ziveri et al., 2023). Betzer et al., (1984) reported that foraminifera calcite is more abundant in northern regions (north
 580 of 42°N) of the western North Pacific. At Ocean Station Papa in the northeast Pacific (50°N , 145°W), model results showed
 581 that foraminifera calcite accounts for only 18–30 % of the total CaCO_3 production, whereas coccolithophores are the major
 582 producer, contributing up to 59–77 % of the total CaCO_3 production (Fabry, 1989). In the Atlantic Ocean, coccolithophore
 583 calcite fluxes and species richness are higher in subtropical than in temperate waters, which is ascribed to the reduced
 584 competition with diatoms in the former (Broerse et al., 2000). Based on these findings, we suggest that differences in ecosystem
 585 structure among sites modulate the relative contribution of various calcifiers to pelagic PIC production. The higher abundance
 586 of non-calcareous phytoplankton (e.g., diatoms) in the transition zone could also reduce coccolithophore biomass via resource
 587 competition (Quere et al., 2005; Sinha et al., 2010) and stimulate the growth of foraminifera (Schiebel et al., 2017), resulting
 588 in the observed decreased contribution of small coccolithophores to total CaCO_3 production.

589

590

591 **Fig. 9.** Pie charts showing the composition of the total calcium carbonate (CaCO_3) standing stock in the upper 150 m of the
 592 water column in the western (this study) and eastern North Pacific Ocean (data from the CDisK-IV cruise; Ziveri et al., 2023).
 593 Red represents the standing stock of large size-fractionated ($>51\text{ }\mu\text{m}$) CaCO_3 from this study, and planktonic foraminifera;



带格式的: 居中

pteropods and heteropods from the CDisK-IV cruise. Blue represents the standing stock of small size-fractionated (1–51 µm) CaCO_3 from this study and coccolithophores from the CDisK-IV cruise.

4.3 CaCO_3 production compared with the eastern North Pacific

While ^{14}C incubations can provide a direct and precise measurement of in situ calcification rates, the calculation method we used offers a practical approach to convert concentration data into production estimates using turnover time (Graziano et al., 2000; Ziveri et al., 2023). This approach has limitations, particularly due to uncertainties in the estimation of coccolithophore calcite, which relies on cell counts and a morphometric-based calcite estimation method, with potential errors reaching up to 50% (Young and Ziveri, 2000; Sheward et al., 2024). The calculation of production rates introduces further uncertainty, as it depends on the coccolithophore calcite standing stock and a broad range of turnover time estimates. Despite these challenges, this method produces reasonable results that are comparable to field observations and thus helps fill a critical data gap in the study region.

Our results indicate that the coccolithophore CaCO_3 production ranged from 0.8 to 2.1 $\text{mmol m}^{-2} \text{d}^{-1}$ during the sampling period, align with globally reported in situ calcification rates and are consistent with observations from the North Atlantic subtropical region (Poulton et al., 2006; Daniels et al., 2018). Although station M30 is located in the oligotrophic NPSG region, it exhibits the highest coccolithophore CaCO_3 production in the euphotic zone of the study area (Fig. 6c). This is primarily because of the deepest euphotic zone at this site, reaching up to 219 m, and the relatively high coccolithophore species diversity. While the coccolithophore abundance at station M30 was lower than at other stations, the less abundant but larger species play an important role in contributing to the CaCO_3 production at this site.

Using a seasonal-correction method (Ziveri et al., 2023), the average coccolithophore CaCO_3 production above 150 m in the euphotic zone was estimated to be $0.350.4 \pm 0.3 \text{ mol m}^{-2} \text{yr}^{-1}$ for the entire research domain, which agrees well with the global estimate of $0.4 \text{ mol m}^{-2} \text{yr}^{-1}$ (Balch et al., 2007) and model result of $0.3 \text{ mol m}^{-2} \text{yr}^{-1}$ in the North Pacific (Hopkins and Balch, 2018). In particular, this production was $0.620.66 \pm 0.2 \text{ mol m}^{-2} \text{yr}^{-1}$ in the subtropical gyre and $0.140.13 \pm 0.1 \text{ mol m}^{-2} \text{yr}^{-1}$ in the Kuroshio-Oyashio transition region (Fig. S2b6d). However, the latter is much lower than the recent estimate of 0.9–1.0 $\text{mol m}^{-2} \text{yr}^{-1}$ by Ziveri et al. (2023) based on data from the transition zone and subpolar gyre in the eastern North Pacific Ocean

using the same seasonal-correction method.

Several factors may lead to the above discrepancy. First, CaCO_3 production rate on the present study was estimated based only on coccolithophores, whereas estimates by Ziveri et al. (2023) also included the contribution from planktonic foraminifera, pteropods and heteropods. Second, in the CDisK-IV cruise to the eastern North Pacific Ocean, coccolithophore calcite concentrations were significantly higher than suspended seawater PIC concentrations collected by in situ pumps in the transition zone and subpolar gyre (Fig. S5S4; Dong et al., 2019, 2022). Calculations based on these apparently inconsistent data may result in an overestimation of actual CaCO_3 production. Third, high spatial and seasonal variations in PIC production might occur between the two oceanic environments, ~~in particular the high dynamics. Particularly, the complex environmental gradients and variability~~ in the ~~Kuroshio-Oyashio~~ transition regions ~~between the subtropical and subpolar gyres~~ may have ~~essentially altered~~ skewed the coccolithophore community and associated CaCO_3 production.

Overall, our results suggest that the calibration of satellite-derived PIC should be unreliable. There was a significant positive relationship between surface coccolithophore calcite concentrations and satellite-derived PIC concentrations ($r^2 = 0.84$; $p < 0.01$; Fig S5a), which implies the latter can reflect the distribution tendency of the former but not the true values, because satellite-derived PIC in high latitude areas is likely overestimated. Over the entire euphotic zone, our results indicate no correlation between satellite-derived PIC concentrations and actual PIC production, a finding that is also highlighted by Ziveri et al. (2023), in which the linear correlation is primarily driven by the highest data value (Fig. S5b). More in situ calcification rates determined by ^{14}C incubations, as well as direct measurements of coccolithophore turnover time, are required to reduce uncertainties in the estimation of PIC production and the assessment of the oceanic CaCO_3 budget.

4.4 Shallow-water CaCO_3 dissolution in the western North Pacific

We used a box model to calculate the magnitude of metabolic CaCO_3 dissolution in shallow waters of the western North Pacific Ocean (Eqs. 3 and 4; Dong et al., 2019, 2022). Focusing on CaCO_3 produced by coccolithophores and assuming that production occurs in the euphotic zone, we applied the model to stations STN43 and STN45 because the calculated metabolic calcite saturation horizon varied from 100 m to 150 m in the Kuroshio-Oyashio transition region. The results suggest that CaCO_3 might start to dissolve in setting marine particles after sinking out of the euphotic zone at the two stations, despite apparently oversaturated ambient conditions (Fig. S6). Three different particle sinking rates (1, 10 and 100 m d^{-1}) were used in our model

calculations (Fig. 10a). To examine the possible influence by lateral transport around the Kuroshio Extension, our data in the upper 1200 m were compared with those obtained during the CDisK-IV cruise (Fig. S5d–f). There was no significant difference in PIC distribution patterns between western and eastern basins across 27°N–42°N in the North Pacific Ocean (one-way ANOVA, $p > 0.05$), with the latter having relatively limited water parcel transport in the horizontal direction. We thus contend that in our first order estimation, the effect of lateral transport on PIC distributions could be considered negligible (Dong et al., 2019; Subhas et al., 2022).

Assuming that all coccolithophore production is exported out of the euphotic zone, our model results show that the PIC sinking flux using the 10 m d^{-1} sinking rate agrees well with data obtained from sediment traps deployed in July 1999 at a 40°N station (Honda et al., 2002) near our research domain (Fig. 10a). At this rate, the R_{TA} driven by Ω_{net} showed a vertical distribution pattern similar to TA^{δ} -chlorofluorocarbon (CFC) age-based R_{TA} in the entire North Pacific Ocean (Feely et al., 2002), with both displaying a maximum at a density of 26.58 kg m^{-3} corresponding to a water depth of 300 m (Fig. 10b). In addition, our R_{TA} varied within a magnitude comparable to Alk^{δ} -transit time distribution (TTD) and ^{14}C age-based R_{TA} values. Instead, those driven by ambient Ω were essentially equal to zero with densities $< 27.0 \text{ kg m}^{-3}$ and became considerable with further increasing densities below 600 m. Therefore, our model results indicate that shallow water CaCO_3 dissolution indeed occurs in the western North Pacific Ocean mainly as a result of metabolic acidification in the particulate microenvironment.

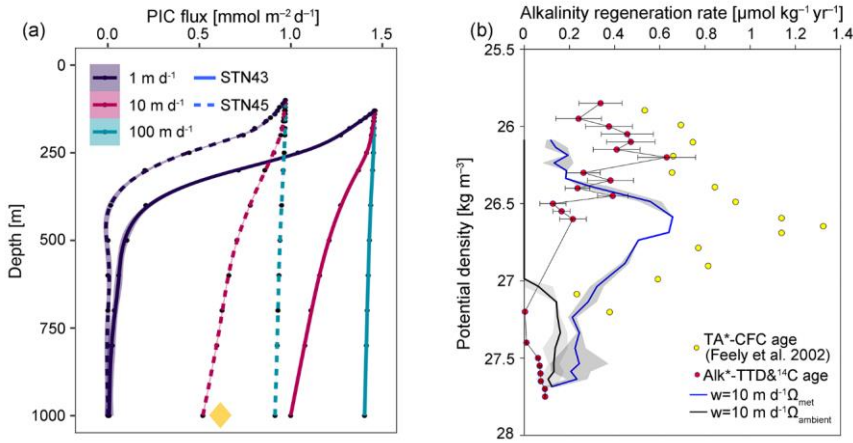


Fig. 10. (a) Particulate inorganic carbon (PIC) fluxes above 1,000 m at stations STN43 and STN45 generated by a box model using three different sinking rates (1, 10 and 100 m d⁻¹); (b) vertical distribution of the alkalinity regeneration rate (R_{TA}) at stations STN43 and STN45 generated by a 1-D model driven by metabolism-altered calcite saturation state (Ω_{met}) and ambient calcite saturation state (Ω_{amb}) at a sinking rate of 10 m d⁻¹. Lines indicate R_{TA} binned and averaged at 0.05 kg m⁻³ potential density intervals. In (a), the yellow diamond marks the PIC flux at 1,000 m at station 40°N, 165°E in the western North Pacific Ocean (Honda et al., 2002; Fig. 1a). In (b), TA*-chlorofluorocarbon (CFC) age represents the excess alkalinity-based R_{TA} from (Feely et al., 2002) and Alk*-TTD&¹⁴C age represents the excess alkalinity-based R_{TA} using transit-time distribution (TTD) ages and ¹⁴C ages combined with Alk* (Key et al., 2004; Gebbie and Huybers, 2012; Carter et al., 2014; Jeansson et al., 2021; Sulpis et al., 2021). Details of the estimation method are provided in the Supplementary Materials.

This finding is consistent with that obtained in the eastern North Pacific Ocean (Subhas et al., 2022), which suggests widely occurring shallow water dissolution throughout the entire North Pacific Ocean associated with organic carbon respiration. The maximum R_{TA} value of 0.66 μmol kg⁻¹ yr⁻¹ at a density of 26.58 kg m⁻³ in our study aligns exactly with that of 0.6 μmol kg⁻¹ yr⁻¹ at a density of 26.54 kg m⁻³ in the eastern North Pacific Ocean (Subhas et al., 2022). It is noteworthy that the R_{TA}

discrepancy between this and previous studies might be ascribed to various dissolution mechanisms (Fig. 10b), since our model only accounted for coccolithophore calcite excluding other calcifying plankton groups such as those producing aragonite and high-Mg calcite. Jansen and Wolf-Gladrow (2001) also suggested that dissolution within zooplankton guts may account for 25 % of the shallow-water dissolution signal.

5 Conclusions

We have demonstrated that coccolithophore abundances and species compositions had distinct geographic and vertical distribution patterns, with *U. tenuis* dominated in the NPSG region while *E. huxleyi* and *Syracosphaera* spp. in the Kuroshio-Oyashio transition region. The environmental variables that best described varying coccolithophore communities were depth and latitude. Calcite derived from coccolithophores contributed on average ~76 % of the PIC standing stocks above 150 m in the euphotic zone, with a relatively greater contribution in the subtropical gyre than in the transition region. Less abundant (<3 %) species such as *C. leptoporus* and *O. fragilis* also made a large contribution of 21 % and 12 % to the coccolithophore calcite concentration in the NPSG region and the Kuroshio-Oyashio transition region, respectively. Our results suggest that coccolithophore CaCO_3 production was 5 fold higher in the former than in the latter, which highlights the importance of coccolithophores in oligotrophic environments. During the sampling period, coccolithophore CaCO_3 production ranged from 0.8 to 2.1 $\text{mmol m}^{-2} \text{d}^{-1}$ in the entire research domain, averaging $1.5 \pm 0.7 \text{ mmol m}^{-2} \text{d}^{-1}$ in the subtropical gyre and $1.2 \pm 0.4 \text{ mmol m}^{-2} \text{d}^{-1}$ in the Kuroshio-Oyashio transition region. This study also inferred that extensive CaCO_3 dissolution occurs above the ambient calcite saturation horizon, and is primarily driven by the metabolic activity associated with organic carbon respiration. Given the important role of CaCO_3 production and dissolution dynamics in the marine alkalinity and carbon cycles, additional studies are required that target coccolithophore production at different scales from seasonal to annual and from regional to global needs further examination, as well as processes leading to CaCO_3 dissolution in the apparently oversaturated upper ocean.

带格式的: 字体: 10 磅, 字体颜色: 文字 1

带格式的: 字体颜色: 文字 1

597 *Data availability.* Data for temperature, salinity, coccolithophore cell and coccolith abundances, coccolithophore calcite ~~and~~,
598 PIC ~~concentrations and nutrients concentrations~~ can be downloaded from the Science Data Bank
599 (~~https://www.scidb.cn/en/s/i6bMFh~~<https://www.scidb.cn/en>). Satellite-based temperature, Chl *a* and PIC concentration data
700 were obtained from the MODIS-Aqua satellite (<https://oceancolor.gsfc.nasa.gov/l3/>).
701

702 *Supplement link.*
703

704 *Author Contributions.* YH, ZC, and MD conceived and designed the study. YH, ZS, DF, and JC contributed to data acquisition
705 and analysis. YH, ZS, ZC, and MD wrote the first draft of the manuscript. YH, ZS, ZC, JY, and MD discussed results and
706 edited the paper. All authors read and approved the final version of the manuscript.
707

708 *Competing interests.* The authors declare that they have no conflict of interests.
709

710 *Disclaimer.*
711

712 *Acknowledgements.* The captain and the crew of R/V *Tan Kah Kee* are acknowledged for their cooperation during the cruise.
713 We thank Feipeng Xu and Xin Liu for providing the chlorophyll *a* data, Lifang Wang, Tao Huang, Yanmin Wang and Zhijie
714 Tan for the nutrient data, Yi Yang and Xianghui Guo for the carbonate system data, Xuchen Wang for advice on particulate
715 inorganic carbon measurements, and Yanping Xu for logistical assistance. Yuye Han was supported by the Joint Training
716 Program in Marine Environmental Sciences sponsored by the China Scholarship Council.
717

718 *Financial support.* This research was funded by the National Natural Science Foundation of China (NSFC project No.
719 42141003, ~~92258302~~ and 42188102). Data and samples were collected onboard the R/V *Tan Kah Kee* implementing the open
720 research cruise NORC2022-306 supported by NSFC Shiptime Sharing Project (project No. 42149303).

721 **References**

- 722 [Armstrong, R. A., Lee, C., Hedges, J. I., Honjo, S., and Wakeham, S. G.: A new, mechanistic model for organic carbon fluxes](#)
723 [in the ocean based on the quantitative association of POC with ballast minerals, Deep sea research II, 49, 219-236,](#)
724 [https://doi.org/10.1016/S0967-0645\(01\)00101-1, 2001.](#)
- 725 [Balch, W., Drapeau, D., Bowler, B., and Booth, E.: Prediction of pelagic calcification rates using satellite measurements, Deep](#)
726 [sea research II, 54, 478-495, https://doi.org/10.1016/j.dsr2.2006.12.006, 2007.](#)
- 727 [Balch, W., Gordon, H. R., Bowler, B., Drapeau, D., and Booth, E.: Calcium carbonate measurements in the surface global](#)
728 [ocean based on Moderate-Resolution Imaging Spectroradiometer data, J Geophys Res-Oceans, 110,](#)
729 [https://doi.org/10.1029/2004jc002560, 2005.](#)
- 730 [Balch, W. M.: The ecology, biogeochemistry, and optical properties of coccolithophores, Annu Rev Mar Sci, 10, 71-98,](#)
731 [https://doi.org/10.1146/annurev-marine-121916-063319, 2018.](#)
- 732 [Balch, W. M., Bowler, B. C., Drapeau, D. T., Lubelczyk, L. C., and Lyczkowski, E.: Vertical distributions of coccolithophores,](#)
733 [PIC, POC, biogenic Silica, and chlorophyll a throughout the global ocean, Global Biogeochem Cy, 32, 2-17,](#)
734 [https://doi.org/10.1002/2016gb005614, 2018.](#)
- 735 [Balch, W. M., Bowler, B. C., Drapeau, D. T., Lubelczyk, L. C., Lyczkowski, E., Mitchell, C., and Wyeth, A.: Coccolithophore](#)
736 [distributions of the north and south Atlantic ocean, Deep sea research I, 151, 103066, https://doi.org/10.1016/j.dsr.2019.06.012,](#)
737 [2019.](#)
- 738 [Balch, W. M., Bates, N. R., Lam, P. J., Twining, B. S., Rosengard, S. Z., Bowler, B. C., Drapeau, D. T., Garley, R., Lubelczyk,](#)
739 [L. C., and Mitchell, C.: Factors regulating the Great Calcite Belt in the Southern Ocean and its biogeochemical significance,](#)
740 [Global Biogeochem Cy, 30, 1124-1144, https://doi.org/10.1002/2016GB005414, 2016.](#)
- 741 [Barrett, P. M., Resing, J. A., Buck, N. J., Feely, R. A., Bullister, J. L., Buck, C. S., and Landing, W. M.: Calcium carbonate](#)
742 [dissolution in the upper 1000 m of the eastern North Atlantic, Global Biogeochem Cy, 28, 386-397,](#)
743 [https://doi.org/10.1002/2013gb004619, 2014.](#)
- 744 [Beaufort, L., Couapel, M., Buchet, N., Claustre, H., and Goyet, C.: Calcite production by coccolithophores in the south east](#)
745 [Pacific Ocean, Biogeosciences, 5, 1101-1117, https://doi.org/10.5194/bg-5-1101-2008, 2008.](#)

[Berelson, W., Balch, W., Najjar, R., Feely, R., Sabine, C., and Lee, K.: Relating estimates of CaCO₃ production, export, and dissolution in the water column to measurements of CaCO₃ rain into sediment traps and dissolution on the sea floor: A revised global carbonate budget, *Global Biogeochem Cy*, 21, <https://doi.org/10.1029/2006gb002803>, 2007.](#)

[Betzer, P., Byrne, R., Acker, J., Lewis, C., Jolley, R., and Feely, R.: The oceanic carbonate system: a reassessment of biogenic controls, *Science*, 226, 1074-1077, <https://doi.org/10.1126/science.226.4678.1074>, 1984.](#)

[Boeckel, B. and Baumann, K.-H.: Vertical and lateral variations in coccolithophore community structure across the subtropical frontal zone in the South Atlantic Ocean, *Mar Micropaleontol*, 67, 255-273, <https://doi.org/10.1016/j.marmicro.2008.01.014>, 2008.](#)

[Bollmann, J., Cortés, M. Y., Haidar, A. T., Brabec, B., Close, A., Hofmann, R., Palma, S., Tupas, L., and Thierstein, H. R.: Techniques for quantitative analyses of calcareous marine phytoplankton, *Mar Micropaleontol*, 44, 163-185, \[https://doi.org/10.1016/s0377-8398\\(01\\)00040-8\]\(https://doi.org/10.1016/s0377-8398\(01\)00040-8\), 2002.](#)

[Brand, L.: Physiological ecology of marine coccolithophores, *Coccolithophores*, 39-50 pp.1994.](#)

[Broecker, W. S. and Peng, T.-H.: Tracers in the Sea, Lamont-Doherty Geological Observatory, Columbia University Palisades, New York, 1982.](#)

[Broerse, A. T., Ziveri, P., van Hinte, J. E., and Honjo, S.: Coccolithophore export production, species composition, and coccolith-CaCO₃ fluxes in the NE Atlantic \(34°N21°W and 48°N21°W\), *Deep sea research II*, 47, 1877-1905, \[https://doi.org/10.1016/s0967-0645\\(00\\)00010-2\]\(https://doi.org/10.1016/s0967-0645\(00\)00010-2\), 2000.](#)

[Brun, P., Vogt, M., Payne, M. R., Gruber, N., O'Brien, C. J., Buitenhuis, E. T., Le Quéré, C., Leblanc, K., and Luo, Y. W.: Ecological niches of open ocean phytoplankton taxa, *Limnol Oceanogr*, 60, 1020-1038, <https://doi.org/10.1002/lno.10074>, 2015.](#)

[Cai, W.-J., Dai, M., Wang, Y., Zhai, W., Huang, T., Chen, S., Zhang, F., Chen, Z., and Wang, Z.: The biogeochemistry of inorganic carbon and nutrients in the Pearl River estuary and the adjacent Northern South China Sea, *Cont Shelf Res*, 24, 1301-1319, <https://doi.org/10.1016/j.csr.2004.04.005>, 2004.](#)

[Cai, W. J., Hu, X., Huang, W. J., Jiang, L. Q., Wang, Y., Peng, T. H., and Zhang, X.: Alkalinity distribution in the western North Atlantic Ocean margins, *J Geophys Res-Oceans*, 115, <https://doi.org/10.1029/2009jc005482>, 2010.](#)

Charalampopoulou, A.: Coccolithophores in high latitude and polar regions: relationships between community composition, calcification and environmental factors, University of Southampton, 2011.

Cornec, M., Laxenaire, R., Speich, S., and Claustre, H.: Impact of mesoscale eddies on deep chlorophyll maxima, *Geophys Res Lett*, 48, e2021GL093470, <https://doi.org/10.1029/2021GL093470>, 2021.

Daniels, C. J., Poulton, A. J., Young, J. R., Esposito, M., Humphreys, M. P., Ribas-Ribas, M., Tynan, E., and Tyrrell, T.: Species-specific calcite production reveals *Coccolithus pelagicus* as the key calcifier in the Arctic Ocean, *Mar Ecol Prog Ser*, 555, 29-47, <https://doi.org/10.3354/meps1182>, 2016.

Daniels, C. J., Poulton, A. J., Balch, W. M., Marañón, E., Adey, T., Bowler, B. C., Cermeño, P., Charalampopoulou, A., Crawford, D. W., and Drapeau, D.: A global compilation of coccolithophore calcification rates, *Earth Syst Sci Data*, 10, 1859-1876, <https://doi.org/10.5194/essd-10-1859-2018>, 2018.

Dean, C. L., Harvey, E. L., Johnson, M. D., and Subhas, A. V.: Microzooplankton grazing on the coccolithophore *Emiliana huxleyi* and its role in the global calcium carbonate cycle, *Science Advances*, 10, eadr5453, <https://doi.org/10.1126/sciadv.adr5453>, 2024.

Deng, Y., Li, P., Fang, T., Jiang, Y., Chen, J., Chen, N., Yuan, D., and Ma, J.: Automated determination of dissolved reactive phosphorus at nanomolar to micromolar levels in natural waters using a portable flow analyzer, *Anal Chem*, 92, 4379-4386, <https://doi.org/10.1021/acs.analchem.9b05252.s001>, 2020.

Dong, S., Wang, X. T., Subhas, A. V., Pavia, F. J., Adkins, J. F., and Berelson, W. M.: Depth profiles of suspended carbon and nitrogen along a North Pacific transect: Concentrations, isotopes, and ratios, *Limnol Oceanogr*, 67, 247-260, <https://doi.org/10.1002/lno.11989>, 2022.

Dong, S., Berelson, W. M., Rollins, N. E., Subhas, A. V., Naviaux, J. D., Celestian, A. J., Liu, X., Turaga, N., Kemnitz, N. J., and Byrne, R. H.: Aragonite dissolution kinetics and calcite/aragonite ratios in sinking and suspended particles in the North Pacific, *Earth Planet Sc Lett*, 515, 1-12, <https://doi.org/10.1016/j.epsl.2019.03.016>, 2019.

Eguchi, N. O., Ujiie, H., Kawahata, H., and Taira, A.: Seasonal variations in planktonic foraminifera at three sediment traps in the subarctic, transition and subtropical zones of the central North Pacific Ocean, *Mar Micropaleontol*, 48, 149-163, [https://doi.org/10.1016/S0377-8398\(03\)00020-3](https://doi.org/10.1016/S0377-8398(03)00020-3), 2003.

796 [Fabry, V. J.: Aragonite production by pteropod molluscs in the subarctic Pacific, Deep sea research I, 36, 1735-1751,](#)
797 [https://doi.org/10.1016/0198-0149\(89\)90069-1](https://doi.org/10.1016/0198-0149(89)90069-1), 1989.

798 [Feely, R., Sabine, C., Lee, K., Millero, F., Lamb, M., Greeley, D., Bullister, J., Key, R., Peng, T. H., and Kozyr, A.: In situ](#)
799 [calcium carbonate dissolution in the Pacific Ocean, Global Biogeochem Cy, 16, 91-91-91-12,](#)
800 <https://doi.org/10.1029/2002gb001866>, 2002.

801 [Feely, R. A., Sabine, C. L., Lee, K., Berelson, W., Kleypas, J., Fabry, V. J., and Millero, F. J.: Impact of anthropogenic CO₂ on](#)
802 [the CaCO₃ system in the oceans, Science, 305, 362-366, https://doi.org/10.1126/science.1097329](#), 2004.

803 [Graziano, L. M., Balch, W. M., Drapeau, D., Bowler, B. C., Vaillancourt, R., and Dunford, S.: Organic and inorganic carbon](#)
804 [production in the Gulf of Maine, Cont Shelf Res, 20, 685-705, https://doi.org/10.1016/S0278-4343\(99\)00091-6](#), 2000.

805 [Gregg, W. W. and Casey, N. W.: Modeling coccolithophores in the global oceans, Deep sea research II, 54, 447-477,](#)
806 <https://doi.org/10.1016/j.dsr2.2006.12.007>, 2007.

807 [Hagino, K., Okada, H., and Matsuoka, H.: Coccolithophore assemblages and morphotypes of *Emiliana huxleyi* in the](#)
808 [boundary zone between the cold Oyashio and warm Kuroshio currents off the coast of Japan, Mar Micropaleontol, 55, 19-47,](#)
809 <https://doi.org/10.1016/j.marmicro.2005.02.002>, 2005.

810 [Hartnett, A., Böttger, L. H., Matzanke, B. F., and Carrano, C. J.: Iron transport and storage in the coccolithophore: *Emiliana*](#)
811 [huxleyi, Metallomics, 4, 1160-1166, https://doi.org/10.1039/c2mt20144e](#), 2012.

812 [Hirata, T., Hardman-Mountford, N., Brewin, R., Aiken, J., Barlow, R., Suzuki, K., Isada, T., Howell, E., Hashioka, T., and](#)
813 [Noguchi-Aita, M.: Synoptic relationships between surface Chlorophyll-a and diagnostic pigments specific to phytoplankton](#)
814 [functional types, Biogeosciences, 8, 311-327, https://doi.org/10.5194/bg-8-311-2011](#), 2011.

815 [Holligan, P., Charalampopoulou, A., and Hutson, R.: Seasonal distributions of the coccolithophore, *Emiliana huxleyi*, and of](#)
816 [particulate inorganic carbon in surface waters of the Scotia Sea, J Marine Syst, 82, 195-205,](#)
817 <https://doi.org/10.1016/j.jmarsys.2010.05.007>, 2010.

818 [Jin, X., Liu, C., Poulton, A. J., Dai, M., and Guo, X.: Coccolithophore responses to environmental variability in the South](#)
819 [China Sea: species composition and calcite content, Biogeosciences, 13, 4843-4861, https://doi.org/10.5194/bg-13-4843-2016,](#)
820 [2016.](#)

Johns, C. T., Bondoc-Naumovitz, K. G., Matthews, A., Matson, P. G., Iglesias-Rodriguez, M. D., Taylor, A. R., Fuchs, H. L., and Bidle, K. D.: Adsorptive exchange of coccolith biominerals facilitates viral infection, *Science Advances*, 9, eadc8728, <https://doi.org/10.1126/sciadv.adc8728>, 2023.

Klaas, C. and Archer, D. E.: Association of sinking organic matter with various types of mineral ballast in the deep sea: Implications for the rain ratio, *Global Biogeochem Cy*, 16, 63-61-63-14, <https://doi.org/10.1029/2001gb001765>, 2002.

Krumhardt, K. M., Lovenduski, N. S., Iglesias-Rodriguez, M. D., and Kleypas, J. A.: Coccolithophore growth and calcification in a changing ocean, *Prog Oceanogr*, 159, 276-295, <https://doi.org/10.1016/j.pocean.2017.10.007>, 2017.

Lai, J., Zou, Y., Zhang, J., and Peres-Neto, P. R.: Generalizing hierarchical and variation partitioning in multiple regression and canonical analyses using the rdacca. hp R package, *Methods Ecol Evol*, 13, 782-788, <https://doi.org/10.1111/2041-210X.13800>, 2022.

Lam, P. J., Ohnemus, D. C., and Auro, M. E.: Size-fractionated major particle composition and concentrations from the US GEOTRACES North Atlantic Zonal Transect, Deep sea research II, 116, 303-320, <https://doi.org/10.1016/j.dsr2.2014.11.020>, 2015.

Lam, P. J., Lee, J.-M., Heller, M. I., Mehic, S., Xiang, Y., and Bates, N. R.: Size-fractionated distributions of suspended particle concentration and major phase composition from the US GEOTRACES Eastern Pacific Zonal Transect (GP16), *Mar Chem*, 201, 90-107, <https://doi.org/10.1016/j.marchem.2017.08.013>, 2018.

Li, Y., Meng, F., Wang, B., Yang, M., Liu, C.-Q., and Xu, S.: Regulation of particulate inorganic carbon by phytoplankton in hydropower reservoirs: Evidence from stable carbon isotope analysis, *Chem Geol*, 579, 120366, <https://doi.org/10.1016/j.chemgeo.2021.120366>, 2021.

Lohbeck, K. T., Riebesell, U., and Reusch, T. B.: Adaptive evolution of a key phytoplankton species to ocean acidification, *Nat Geosci*, 5, 346-351, <https://doi.org/10.1038/ngeo1441>, 2012.

Ma, D., Gregor, L., and Gruber, N.: Four decades of trends and drivers of global surface ocean acidification, *Global Biogeochem Cy*, 37, e2023GB007765, <https://doi.org/10.1029/2023GB007765>, 2023.

Maranón, E., Balch, W. M., Cermeno, P., González, N., Sobrino, C., Fernández, A., Huete-Ortega, M., López-Sandoval, D. C., Delgado, M., and Estrada, M.: Coccolithophore calcification is independent of carbonate chemistry in the tropical ocean,

846 [Limnol Oceanogr](https://doi.org/10.1002/lno.10295), 61, 1345-1357, <https://doi.org/10.1002/lno.10295>, 2016.

847 [Naviaux, J. D., Subhas, A. V., Rollins, N. E., Dong, S., Berelson, W. M., and Adkins, J. F.: Temperature dependence of calcite](#)

848 [dissolution kinetics in seawater, *Geochim Cosmochim Acta*, 246, 363-384, <https://doi.org/10.1016/j.gca.2018.11.037>, 2019.](#)

849 [Neukermans, G., Bach, L., Butterley, A., Sun, Q., Claustre, H., and Fournier, G.: Quantitative and mechanistic understanding](#)

850 [of the open ocean carbonate pump-perspectives for remote sensing and autonomous in situ observation, *Earth-Science Reviews*,](#)

851 [239, 104359, <https://doi.org/10.1016/j.earscirev.2023.104359>, 2023.](#)

852 [O'Brien, C. J., Vogt, M., and Gruber, N.: Global coccolithophore diversity: Drivers and future change, *Prog Oceanogr*, 140,](#)

853 [27-42, <https://doi.org/10.1016/j.pocean.2015.10.003>, 2016.](#)

854 [Okada, H. and Honjo, S.: The distribution of oceanic coccolithophorids in the Pacific, *Deep Sea Research and Oceanographic*](#)

855 [Abstracts](#), 355-374, 10.1016/0011-7471(73)90059-4, 1973.

856 [Oksanen, J.: Vegan: community ecology package, <http://vegan.r-forge.r-project.org/>, 2010.](#)

857 [Poulton, A., Sanders, R., Holligan, P., Stinchcombe, M., Adey, T., Brown, L., and Chamberlain, K.: Phytoplankton](#)

858 [mineralization in the tropical and subtropical Atlantic Ocean, *Global Biogeochem Cy*, 20,](#)

859 [https://doi.org/10.1029/2006gb002712, 2006.](#)

860 [Poulton, A. J., Holligan, P. M., Charalampopoulou, A., and Adey, T. R.: Coccolithophore ecology in the tropical and subtropical](#)

861 [Atlantic Ocean: New perspectives from the Atlantic meridional transect \(AMT\) programme, *Prog Oceanogr*, 158, 150-170,](#)

862 [https://doi.org/10.1016/j.pocean.2017.01.003, 2017.](#)

863 [Poulton, A. J., Painter, S. C., Young, J. R., Bates, N. R., Bowler, B., Drapeau, D., Lyczskowski, E., and Balch, W. M.: The](#)

864 [2008 *Emiliana huxleyi* bloom along the Patagonian Shelf: Ecology, biogeochemistry, and cellular calcification, *Global*](#)

865 [Biogeochem Cy](#), 27, 1023-1033, <https://doi.org/10.1002/2013gb004641>, 2013.

866 [Quere, C. L., Harrison, S. P., Colin Prentice, I., Buitenhuis, E. T., Aumont, O., Bopp, L., Claustre, H., Cotrim Da Cunha, L.,](#)

867 [Geider, R., and Giraud, X.: Ecosystem dynamics based on plankton functional types for global ocean biogeochemistry models,](#)

868 [Global Change Biol](#), 11, 2016-2040, <https://doi.org/10.1111/j.1365-2486.2005.1004.x>, 2005.

869 [Raven, J. A. and Crawford, K.: Environmental controls on coccolithophore calcification, *Mar Ecol Prog Ser*, 470, 137-166,](#)

870 [https://doi.org/10.3354/meps09993, 2012.](#)

871 [Rickaby, R., Monteiro, F., Bach, L., Brownlee, C., Bown, P., Poulton, A., Beaufort, L., Dutkiewicz, S., Gibbs, S., and Gutowska,](#)
 872 [M.: Why marine phytoplankton calcify, Science Advances, 2, <https://doi.org/10.1126/sciadv.1501822>, 2016a.](#)
 873 [Rickaby, R. E., Hermoso, M., Lee, R. B., Rae, B. D., Heures, A. M., Balestreri, C., Chakravarti, L., Schroeder, D. C., and](#)
 874 [Brownlee, C.: Environmental carbonate chemistry selects for phenotype of recently isolated strains of *Emiliania huxleyi*, Deep](#)
 875 [sea research II, 127, 28-40, <https://doi.org/10.1016/j.dsr2.2016.02.010>, 2016b.](#)
 876 [Rigual Hernández, A. S., Trull, T. W., Nodder, S. D., Flores, J. A., Bostock, H., Abrantes, F., Eriksen, R. S., Sierro, F. J., Davies,](#)
 877 [D. M., and Ballegeer, A.-M.: Coccolithophore biodiversity controls carbonate export in the Southern Ocean, Biogeosciences,](#)
 878 [17, 245-263, <https://doi.org/10.5194/bg-17-245-2020>, 2020.](#)
 879 [Rivero-Calle, S., Gnanadesikan, A., Del Castillo, C. E., Balch, W. M., and Guikema, S. D.: Multidecadal increase in North](#)
 880 [Atlantic coccolithophores and the potential role of rising CO₂, Science, 350, 1533-1537,](#)
 881 [https://doi.org/10.1126/science.aaa8026, 2015.](#)
 882 [Rousseaux, C. S. and Gregg, W. W.: Recent decadal trends in global phytoplankton composition, Global Biogeochem Cy, 29,](#)
 883 [1674-1688, <https://doi.org/10.1002/2015gb005139>, 2015.](#)
 884 [Saavedra-Pellitero, M., Baumann, K.-H., Flores, J.-A., and Gersonde, R.: Biogeographic distribution of living](#)
 885 [coccolithophores in the Pacific sector of the Southern Ocean, Mar Micropaleontol, 109, 1-20,](#)
 886 [https://doi.org/10.1016/j.marmicro.2014.03.003, 2014.](#)
 887 [Schiebel, R., Spielhagen, R. F., Garnier, J., Hagemann, J., Howa, H., Jentzen, A., Martínez-García, A., Meilland, J., Michel,](#)
 888 [E., and Repschläger, J.: Modern planktic foraminifers in the high-latitude ocean, Mar Micropaleontol, 136, 1-13,](#)
 889 [https://doi.org/10.1016/j.marmicro.2017.08.004, 2017.](#)
 890 [Schlüter, L., Lohbeck, K. T., Gutowska, M. A., Gröger, J. P., Riebesell, U., and Reusch, T. B.: Adaptation of a globally](#)
 891 [important coccolithophore to ocean warming and acidification, Nat Clim Change, 4, 1024-1030,](#)
 892 [https://doi.org/10.1038/nclimate2379, 2014.](#)
 893 [Sheward, R. M., Poulton, A. J., Young, J. R., de Vries, J., Monteiro, F. M., and Herrle, J. O.: Cellular morphological trait](#)
 894 [dataset for extant coccolithophores from the Atlantic Ocean, Scientific Data, 11, 720, \[https://doi.org/10.1038/s41597-024-\]\(https://doi.org/10.1038/s41597-024-03544-1\)](#)
 895 [03544-1, 2024.](#)

896 [Sinha, B., Buitenhuis, E. T., Le Quéré, C., and Anderson, T. R.: Comparison of the emergent behavior of a complex ecosystem](#)
897 [model in two ocean general circulation models, Prog Oceanogr, 84, 204-224, <https://doi.org/10.1016/j.pocean.2009.10.003>,](#)
898 [2010.](#)

899 [Smith, S. V. and Mackenzie, F. T.: The role of CaCO₃ reactions in the contemporary oceanic CO₂ cycle, Aquat Geochem,](#)
900 [22, 153-175, <https://doi.org/10.1007/s10498-015-9282-y>, 2016.](#)

901 [Subhas, A. V., Dong, S., Naviaux, J. D., Rollins, N. E., Ziveri, P., Gray, W., Rae, J. W., Liu, X., Byrne, R. H., and Chen, S.:](#)
902 [Shallow calcium carbonate cycling in the North Pacific Ocean, Global Biogeochem Cy, 36, e2022GB007388,](#)
903 [https://doi.org/10.7185/gold2021.4474, 2022.](#)

904 [Sugie, K. and Suzuki, K.: Characterization of the synoptic-scale diversity, biogeography, and size distribution of diatoms in](#)
905 [the North Pacific, Limnol Oceanogr, 62, 884-897, <https://doi.org/10.1002/lno.10473>, 2017.](#)

906 [Takahashi, T., Sutherland, S. C., Wanninkhof, R., Sweeney, C., Feely, R. A., Chipman, D. W., Hales, B., Friederich, G., Chavez,](#)
907 [F., and Sabine, C.: Climatological mean and decadal change in surface ocean pCO₂, and net sea–air CO₂ flux over the global](#)
908 [oceans, Deep sea research II, 56, 554-577, <https://doi.org/10.1016/j.dsr2.2008.12.009>, 2009.](#)

909 [Taylor, A. R., Brownlee, C., and Wheeler, G.: Coccolithophore cell biology: chalking up progress, Annu Rev Mar Sci, 9, 283-](#)
910 [310, <https://doi.org/10.1146/annurev-marine-122414-034032>, 2017.](#)

911 [Taylor, B. J., Rae, J. W., Gray, W. R., Darling, K. F., Burke, A., Gersonde, R., Abelman, A., Maier, E., Esper, O., and Ziveri,](#)
912 [P.: Distribution and ecology of planktic foraminifera in the North Pacific: Implications for paleo-reconstructions, Quaternary](#)
913 [Sci Rev, 191, 256-274, <https://doi.org/10.1016/j.quascirev.2018.05.006>, 2018.](#)

914 [Vincent, F., Gralka, M., Schleyer, G., Schatz, D., Cabrera-Brufau, M., Kuhlisch, C., Sichert, A., Vidal-Melgosa, S., Mayers,](#)
915 [K., Barak-Gavish, N., Flores, J. M., Masdeu-Navarro, M., Egge, J. K., Larsen, A., Hehemann, J.-H., Marrasé, C., Simó, R.,](#)
916 [Cordero, O. X., and Vardi, A.: Viral infection switches the balance between bacterial and eukaryotic recyclers of organic matter](#)
917 [during coccolithophore blooms, Nat Commun, 14, 510, <https://doi.org/10.1038/s41467-023-36049-3>, 2023.](#)

918 [Volk, T. and Hoffert, M. I.: Ocean carbon pumps: Analysis of relative strengths and efficiencies in ocean-driven atmospheric](#)
919 [CO₂ changes, The carbon cycle and atmospheric CO₂: Natural variations Archean to present, 32, 99-110,](#)
920 [https://doi.org/10.1029/gm032p0099, 1985.](#)

Welschmeyer, N. A.: Fluorometric analysis of chlorophyll a in the presence of chlorophyll b and pheopigments, *Limnol Oceanogr.* 39, 1985-1992, <https://doi.org/10.4319/lo.1994.39.8.1985>, 1994.

Yang, T.-N. and Wei, K.-Y.: How many coccoliths are there in a coccosphere of the extant coccolithophorids? A compilation, *Br. Phycol. J.* 26, 67-80, <https://doi.org/10.58998/jnr2275>, 2003.

Young, J., Geisen, M., Cros, L., Kleijne, A., Sprengel, C., Probert, I., and Østergaard, J.: A guide to extant coccolithophore taxonomy, *Journal of Nannoplankton Research*, 1, 1-132, <https://doi.org/10.58998/jnr2297>, 2003.

Coccolith2 Macros, available at: ina.tmsoc.org/nannos/coccolith2/Usernotes.html: <http://ina.tmsoc.org/nannos/coccolith2/Usernotes.html>, last

Young, J. R. and Ziveri, P.: Calculation of coccolith volume and its use in calibration of carbonate flux estimates, *Deep sea research II*, 47, 1679-1700, [https://doi.org/10.1016/s0967-0645\(00\)00003-5](https://doi.org/10.1016/s0967-0645(00)00003-5), 2000.

Zhang, J.-Z.: Shipboard automated determination of trace concentrations of nitrite and nitrate in oligotrophic water by gas-segmented continuous flow analysis with a liquid waveguide capillary flow cell, *Deep sea research I*, 47, 1157-1171, [https://doi.org/10.1016/s0967-0637\(99\)00085-0](https://doi.org/10.1016/s0967-0637(99)00085-0), 2000.

Zhu, Y., Yuan, D., Huang, Y., Ma, J., and Feng, S.: A sensitive flow-batch system for on board determination of ultra-trace ammonium in seawater: Method development and shipboard application, *Anal Chim Acta*, 794, 47-54, <https://doi.org/10.1016/j.aca.2013.08.009>, 2013.

Zhu, Y., Liu, J., Huang, T., Wang, L., Trull, T. W., and Dai, M.: On the fluorometric measurement of ammonium in oligotrophic seawater: Assessment of reagent blanks and interferences, *Limnol Oceanogr-Meth*, 16, 516-524, <https://doi.org/10.1002/lom3.10263>, 2018.

Ziveri, P., de Bernardi, B., Baumann, K.-H., Stoll, H. M., and Mortyn, P. G.: Sinking of coccolith carbonate and potential contribution to organic carbon ballasting in the deep ocean, *Deep sea research II*, 54, 659-675, <https://doi.org/10.1016/j.dsr2.2007.01.006>, 2007.

Ziveri, P., Gray, W. R., Anglada-Ortiz, G., Manno, C., Grellaud, M., Incarbona, A., Rae, J. W. B., Subhas, A. V., Pallacks, S., and White, A.: Pelagic calcium carbonate production and shallow dissolution in the North Pacific Ocean, *Nat Commun*, 14, 805, <https://doi.org/10.1038/s41467-023-36177-w>, 2023.

Anderson, L. A., and Sarmiento, J. L.: Redfield ratios of remineralization determined by nutrient data analysis, *Global biogeochemical cycles*, 8, 65–80, <https://doi.org/10.1029/93gb03318>, 1994.

Armstrong, R. A., Lee, C., Hedges, J. I., Honjo, S., and Wakeham, S. G.: A new, mechanistic model for organic carbon fluxes in the ocean based on the quantitative association of POC with ballast minerals, *Deep Sea Research II*, 49, 219–236, [https://doi.org/10.1016/S0967-0645\(01\)00101-1](https://doi.org/10.1016/S0967-0645(01)00101-1), 2001.

Baleh, W., Drapeau, D., Bowler, B., and Booth, E.: Prediction of pelagic calcification rates using satellite measurements, *Deep Sea Research II*, 54, 478–495, <https://doi.org/10.1016/j.dsr2.2006.12.006>, 2007.

Baleh, W., Gordon, H. R., Bowler, B., Drapeau, D., and Booth, E.: Calcium carbonate measurements in the surface global ocean based on Moderate-Resolution Imaging Spectroradiometer data, *Journal of Geophysical Research: Oceans*, 110, <https://doi.org/10.1029/2004je002560>, 2005.

Baleh, W. M.: The ecology, biogeochemistry, and optical properties of coccolithophores, *Annual review of marine science*, 10, 71–98, <https://doi.org/10.1146/annurev-marine-121916-063319>, 2018.

Baleh, W. M., Bowler, B. C., Drapeau, D. T., Lubelezyk, L. C., Lyezkowski, E.: Vertical distributions of coccolithophores, PIC, POC, biogenic Silica, and chlorophyll *a* throughout the global ocean, *Global Biogeochemical Cycles*, 32, 2–17, <https://doi.org/10.1002/2016gb005614>, 2018.

Baleh, W. M., Bowler, B. C., Drapeau, D. T., Lubelezyk, L. C., Lyezkowski, E., Mitchell, C., and Wyeth, A.: Coccolithophore distributions of the north and south Atlantic ocean, *Deep Sea Research I*, 151, 103066, <https://doi.org/10.1016/j.dsr.2019.06.012>, 2019.

Barrett, P. M., Resing, J. A., Buck, N. J., Feely, R. A., Bullister, J. L., Buck, C. S., and Landing, W. M.: Calcium carbonate dissolution in the upper 1000 m of the eastern North Atlantic, *Global biogeochemical cycles*, 28, 386–397, <https://doi.org/10.1002/2013gb004619>, 2014.

Beaufort, L., Couapel, M., Buchet, N., Claustre, H., and Goyet, C.: Calcite production by coccolithophores in the south-east Pacific Ocean, *Biogeosciences*, 5, 1101–1117, <https://doi.org/10.5194/bg-5-1101-2008>, 2008.

Berelson, W., Baleh, W., Najjar, R., Feely, R., Sabine, C., and Lee, K.: Relating estimates of CaCO_3 production, export, and dissolution in the water column to measurements of CaCO_3 rain into sediment traps and dissolution on the sea floor: A revised

global carbonate budget, *Global Biogeochemical Cycles*, 21, <https://doi.org/10.1029/2006gb002803>, 2007.

Betzler, P., Byrne, R., Acker, J., Lewis, C., Jolley, R., and Feely, R.: The oceanic carbonate system: a reassessment of biogenic controls, *Science*, 226, 1074–1077, <https://doi.org/10.1126/science.226.4678.1074>, 1984.

Beuvier, T., Probert, I., Beaufort, L., Suchéras-Marx, B., Chushkin, Y., Zontone, F., and Gibaud, A.: X-ray nanotomography of coccolithophores reveals that coccolith mass and segment number correlate with grid size, *Nature communications*, 10, 751, <https://doi.org/10.1038/s41467-019-08635-x>, 2019.

Bishop, J. K., Collier, R. W., Kettens, D. R., and Edmond, J. M.: The chemistry, biology, and vertical flux of particulate matter from the upper 1500 m of the Panama Basin, *Deep Sea Research I*, 27, 615–640, [https://doi.org/10.1016/0198-0149\(80\)90077-1](https://doi.org/10.1016/0198-0149(80)90077-1), 1980.

Boeckel, B. and Baumann, K.-H.: Vertical and lateral variations in coccolithophore community structure across the subtropical frontal zone in the South Atlantic Ocean, *Marine micropaleontology*, 67, 255–273, <https://doi.org/10.1016/j.marmicro.2008.01.014>, 2008.

Bollmann, J., Cortés, M. Y., Haidar, A. T., Bräse, B., Close, A., Hofmann, R., Palma, S., Tupas, L., and Thierstein, H. R.: Techniques for quantitative analyses of calcareous marine phytoplankton, *Marine Micropaleontology*, 44, 163–185, [https://doi.org/10.1016/s0377-8398\(01\)00040-8](https://doi.org/10.1016/s0377-8398(01)00040-8), 2002.

Brand, L.: Physiological ecology of marine coccolithophores, *Coccolithophores*, 39–50 pp. 1994.

Broecker, W. S. and Peng, T. H.: *Tracers in the Sea*, Lamont-Doherty Geological Observatory, Columbia University Palisades, New York, 1982.

Broerse, A. T., Ziveri, P., van Hinte, J. E., and Honjo, S.: Coccolithophore export production, species composition, and coccolith-CaCO₃ fluxes in the NE Atlantic (34°N21°W and 48°N21°W), *Deep Sea Research II*, 47, 1877–1905, [https://doi.org/10.1016/s0967-0645\(00\)00010-2](https://doi.org/10.1016/s0967-0645(00)00010-2), 2000.

Brun, P., Vogt, M., Payne, M. R., Gruber, N., O'Brien, C. J., Buitenhuis, E. T., Le Quéré, C., Leblanc, K., and Luo, Y. W.: Ecological niches of open ocean phytoplankton taxa, *Limnology and Oceanography*, 60, 1020–1038, <https://doi.org/10.1002/lno.10074>, 2015.

Cao, Z. and Dai, M.: Shallow-depth CaCO₃ dissolution: Evidence from excess calcium in the South China Sea and its export

to the Pacific Ocean, *Global Biogeochemical Cycles*, 25, <https://doi.org/10.1029/2009gb003690>, 2011.

Carter, B. R., Toggweiler, J., Key, R. M., and Sarmiento, J. L.: Processes determining the marine alkalinity and calcium carbonate saturation state distributions, *Biogeosciences*, 11, 7349–7362, <https://doi.org/10.5194/bg-11-7349-2014>, 2014.

Charalampopoulou, A.: *Coccolithophores in high-latitude and polar regions: relationships between community composition, calcification and environmental factors*, University of Southampton, 2011.

Chung, S. N., Lee, K., Feely, R., Sabine, C., Millero, F., Wanninkhof, R., Bullister, J., Key, R., and Peng, T. H.: Calcium carbonate budget in the Atlantic Ocean based on water column inorganic carbon chemistry, *Global Biogeochemical Cycles*, 17, <https://doi.org/10.1029/2002gb002001>, 2003.

Daniels, C. J., Poulton, A. J., Young, J. R., Esposito, M., Humphreys, M. P., Ribas-Ribas, M., Tynan, E., and Tyrrell, T.: Species-specific calcite production reveals *Coccolithus pelagicus* as the key calcifier in the Arctic Ocean, *Marine Ecology Progress Series*, 555, 29–47, <https://doi.org/10.3354/meps1182>, 2016.

Dong, S., Wang, X. T., Subhas, A. V., Pavia, F. J., Adkins, J. F., and Berelson, W. M.: Depth profiles of suspended carbon and nitrogen along a North Pacific transect: Concentrations, isotopes, and ratios, *Limnology and Oceanography*, 67, 247–260, <https://doi.org/10.1002/lno.11989>, 2022.

Dong, S., Berelson, W. M., Rollins, N. E., Subhas, A. V., Naviaux, J. D., Celestian, A. J., Liu, X., Turaga, N., Kemnitz, N. J., and Byrne, R. H.: Aragonite dissolution kinetics and calcite/aragonite ratios in sinking and suspended particles in the North Pacific, *Earth and Planetary Science Letters*, 515, 1–12, <https://doi.org/10.1016/j.epsl.2019.03.016>, 2019.

Fabry, V. J.: Aragonite production by pteropod molluscs in the subarctic Pacific, *Deep Sea Research I*, 36, 1735–1751, [https://doi.org/10.1016/0198-0149\(89\)90069-1](https://doi.org/10.1016/0198-0149(89)90069-1), 1989.

Feely, R., Sabine, C., Lee, K., Millero, F., Lamb, M., Greeley, D., Bullister, J., Key, R., Peng, T. H., and Kozyr, A.: In situ calcium carbonate dissolution in the Pacific Ocean, *Global Biogeochemical Cycles*, 16, 91–91–91–12, <https://doi.org/10.1029/2002gb001866>, 2002.

Feely, R. A., Sabine, C. L., Lee, K., Berelson, W., Kleypas, J., Fabry, V. J., and Millero, F. J.: Impact of anthropogenic CO₂ on the CaCO₃ system in the oceans, *Science*, 305, 362–366, <https://doi.org/10.1126/science.1097329>, 2004.

Folkerts, E. J., Oehlert, A. M., Heuer, R. M., Nixon, S., Stieglitz, J. D., and Grosell, M.: The role of marine fish-produced

carbonates in the oceanic carbon cycle is determined by size, specific gravity, and dissolution rate, *Science of The Total Environment*, 916, 170044, <https://doi.org/10.1016/j.scitotenv.2024.170044>, 2024.

Gebbie, G. and Huybers, P.: The mean age of ocean waters inferred from radiocarbon observations: Sensitivity to surface sources and accounting for mixing histories, *Journal of Physical Oceanography*, 42, 291–305, <https://doi.org/10.1175/jpo-d-11-043.1>, 2012.

Gregg, W. W. and Casey, N. W.: Modeling coccolithophores in the global oceans, *Deep Sea Research II*, 54, 447–477, <https://doi.org/10.1016/j.dsr2.2006.12.007>, 2007.

Hagino, K., Okada, H., and Matsuoka, H.: Coccolithophore assemblages and morphotypes of *Emiliania huxleyi* in the boundary zone between the cold Oyashio and warm Kuroshio currents off the coast of Japan, *Marine Micropaleontology*, 55, 19–47, <https://doi.org/10.1016/j.marmicro.2005.02.002>, 2005.

Hoffmann, H.: violin-m: Simple violin plot using matlab default kernel density estimation, 2015.

Honda, M. C., Imai, K., Nojiri, Y., Hoshi, F., Sugawara, T., and Kusakabe, M.: The biological pump in the northwestern North Pacific based on fluxes and major components of particulate matter obtained by sediment trap experiments (1997–2000), *Deep Sea Research II*, 49, 5595–5625, [https://doi.org/10.1016/S0967-0645\(02\)00201-1](https://doi.org/10.1016/S0967-0645(02)00201-1), 2002.

Honjo, S., Manganini, S. J., Krishfield, R. A., and Francois, R.: Particulate organic carbon fluxes to the ocean interior and factors controlling the biological pump: A synthesis of global sediment trap programs since 1983, *Progress in Oceanography*, 76, 217–285, <https://doi.org/10.1016/j.pocean.2007.11.003>, 2008.

Hopkins, J. and Balch, W. M.: A new approach to estimating coccolithophore calcification rates from space, *Journal of Geophysical Research: Biogeosciences*, 123, 1447–1459, <https://doi.org/10.1016/j.dsr2.2007.01.006>, 2018.

Jansson, E., Steinfeldt, R., and Tanhua, T.: Water mass ages based on GLODAPv2 data product (NCEI Accession 0226793), 2021.

Jin, X., Liu, C., Xu, J., and Guo, X.: Coccolithophore abundance, degree of calcification, and their contribution to particulate inorganic carbon in the South China Sea, *Journal of Geophysical Research: Biogeosciences*, 127, e2021JG006657, <https://doi.org/10.1029/2021jg006657>, 2022.

Key, R. M., Kozyr, A., Sabine, C. L., Lee, K., Wanninkhof, R., Bullister, J. L., Feely, R. A., Millero, F. J., Mordy, C., and Peng,

T. H.: A global ocean carbon climatology: Results from Global Data Analysis Project (GLODAP), *Global biogeochemical cycles*, 18, <https://doi.org/10.1029/2004gb002247>, 2004.

Klaas, C. and Archer, D. E.: Association of sinking organic matter with various types of mineral ballast in the deep sea: Implications for the rain ratio, *Global Biogeochemical Cycles*, 16, 63–61–63–14, <https://doi.org/10.1029/2001gb001765>, 2002.

Krumhardt, K. M., Lovenduski, N. S., Iglesias-Rodriguez, M. D., and Kleypas, J. A.: Coccolithophore growth and calcification in a changing ocean, *Progress in oceanography*, 159, 276–295, <https://doi.org/10.1016/j.pocean.2017.10.007>, 2017.

Lai, J., Zou, Y., Zhang, J., and Peres-Neto, P. R.: Generalizing hierarchical and variation partitioning in multiple regression and canonical analyses using the rdaaep R package, *Methods in Ecology and Evolution*, 13, 782–788, <https://doi.org/10.1111/2041-210X.13800>, 2022.

Lam, P. J., Ohnemus, D. C., and Auro, M. E.: Size-fractionated major particle composition and concentrations from the US GEOTRACES North Atlantic Zonal Transect, Deep Sea Research II, 116, 303–320, <https://doi.org/10.1016/j.dsr2.2014.11.020>, 2015.

Lam, P. J., Lee, J. M., Heller, M. I., Mehie, S., Xiang, Y., and Bates, N. R.: Size-fractionated distributions of suspended particle concentration and major phase composition from the US GEOTRACES Eastern Pacific Zonal Transect (GP16), *Marine Chemistry*, 201, 90–107, <https://doi.org/10.1016/j.marchem.2017.08.013>, 2018.

Li, Y., Meng, F., Wang, B., Yang, M., Liu, C. Q., and Xu, S.: Regulation of particulate inorganic carbon by phytoplankton in hydropower reservoirs: Evidence from stable carbon isotope analysis, *Chemical Geology*, 579, 120366, <https://doi.org/10.1016/j.chemgeo.2021.120366>, 2021.

Liaw, A. and Wiener, M.: Classification and regression by randomForest, *R news*, 2, 18–22, 2002.

Maranón, E., Balch, W. M., Cermeno, P., González, N., Sobrino, C., Fernández, A., Huete-Ortega, M., López-Sandoval, D. C., Delgado, M., and Estrada, M.: Coccolithophore calcification is independent of carbonate chemistry in the tropical ocean, *Limnology and Oceanography*, 61, 1345–1357, <https://doi.org/10.1002/lno.10295>, 2016.

Milliman, J., Troy, P., Balch, W., Adams, A., Li, Y.-H., and Mackenzie, F.: Biologically mediated dissolution of calcium carbonate above the chemical lysocline?, *Deep Sea Research I*, 46, 1653–1669, [https://doi.org/10.1016/s0967-0637\(99\)00034-5](https://doi.org/10.1016/s0967-0637(99)00034-5), 1999.

Naviaux, J. D., Subhas, A. V., Rollins, N. E., Dong, S., Berelson, W. M., and Adkins, J. F.: Temperature dependence of calcite dissolution kinetics in seawater, *Geochimica et Cosmochimica Acta*, 246, 363–384, <https://doi.org/10.1016/j.gca.2018.11.037>, 2019.

O'Brien, C. J., Vogt, M., and Gruber, N.: Global coccolithophore diversity: Drivers and future change, *Progress in Oceanography*, 140, 27–42, <https://doi.org/10.1016/j.pocean.2015.10.003>, 2016.

Oehlert, A. M., Garza, J., Nixon, S., Frank, L., Folkerts, E. J., Stieglitz, J. D., Lu, C., Heuer, R. M., Benetti, D. D., and Del Campo, J.: Implications of dietary carbon incorporation in fish carbonates for the global carbon cycle, *Science of The Total Environment*, 916, 169895, <https://doi.org/10.1016/j.scitotenv.2024.169895>, 2024.

Okada, H. and Honjo, S.: The distribution of oceanic coccolithophorids in the Pacific, *Deep Sea Research and Oceanographic Abstracts*, 355–374, [https://doi.org/10.1016/0011-7471\(73\)90059-4](https://doi.org/10.1016/0011-7471(73)90059-4), 1973.

Oksanen, J., Kindt, R., Legendre, P., O'hara, B., Stevens, M., Oksanen, M., and Suggests, M.: The vegan package: community ecology package, R package version, 1, 1–190, 2007.

Pond, D., Harris, R., and Brownlee, C.: A microinjection technique using a pH-sensitive dye to determine the gut pH of *Calanus helgolandicus*, *Marine Biology*, 123, 75–79, <https://doi.org/10.1007/BF00350325>, 1995.

Poulton, A., Sanders, R., Holligan, P., Stincheombe, M., Adey, T., Brown, L., and Chamberlain, K.: Phytoplankton mineralization in the tropical and subtropical Atlantic Ocean, *Global Biogeochemical Cycles*, 20, <https://doi.org/10.1029/2006gb002712>, 2006.

Poulton, A. J., Painter, S. C., Young, J. R., Bates, N. R., Bowler, B., Drapeau, D., Lyeżsekowski, E., and Balch, W. M.: The 2008 *Emiliania huxleyi* bloom along the Patagonian Shelf: Ecology, biogeochemistry, and cellular calcification, *Global Biogeochemical Cycles*, 27, 1023–1033, <https://doi.org/10.1002/2013gb004641>, 2013.

Quere, C. L., Harrison, S. P., Colin Prentice, I., Buitenhuis, E. T., Aumont, O., Bopp, L., Claustre, H., Cotrim Da Cunha, L., Geider, R., and Giraud, X.: Ecosystem dynamics based on plankton functional types for global ocean biogeochemistry models, *Global Change Biology*, 11, 2016–2040, <https://doi.org/10.1111/j.1365-2486.2005.1004.x>, 2005.

Rigual Hernández, A. S., Trull, T. W., Nodder, S. D., Flores, J. A., Bostock, H., Abrantes, F., Eriksen, R. S., Sierro, F. J., Davies, D. M., and Ballegeer, A. M.: Coccolithophore biodiversity controls carbonate export in the Southern Ocean, *Biogeosciences*,

1096 17, 245–263, <https://doi.org/10.5194/bg-17-245-2020>, 2020.

1097 Rivero-Calle, S., Gnanadesikan, A., Del Castillo, C. E., Balch, W. M., and Guikema, S. D.: Multidecadal increase in North

1098 Atlantic coccolithophores and the potential role of rising CO₂, *Science*, 350, 1533–1537,

1099 <https://doi.org/10.1126/science.aaa8026>, 2015.

1100 Roca-Martí, M., Benitez-Nelson, C. R., Umhau, B. P., Wyatt, A. M., Clevenger, S. J., Pike, S., Horner, T. J., Estapa, M. L.,

1101 Resplandy, L., and Buesseler, K. O.: Concentrations, ratios, and sinking fluxes of major bioelements at Ocean Station Papa,

1102 *Elem-Sci-Anth*, 9, 00166, <https://doi.org/10.1525/elementa.2020.00166>, 2021.

1103 Rousseaux, C. S. and Gregg, W. W.: Recent decadal trends in global phytoplankton composition, *Global Biogeochemical*

1104 *Cycles*, 29, 1674–1688, <https://doi.org/10.1002/2015gb005139>, 2015.

1105 Saavedra-Pellitero, M., Baumann, K. H., Flores, J. A., and Gersonde, R.: Biogeographic distribution of living

1106 coccolithophores in the Pacific sector of the Southern Ocean, *Marine Micropaleontology*, 109, 1–20,

1107 <https://doi.org/10.1016/j.marmicro.2014.03.003>, 2014.

1108 Sabine, C., Feely, R., Key, R., Bullister, J., Millero, F., Lee, K., Peng, T. H., Tilbrook, B., Ono, T., and Wong, C.: Distribution

1109 of anthropogenic CO₂ in the Pacific Ocean, *Global Biogeochemical Cycles*, 16, 30–31–30–17,

1110 <https://doi.org/10.1007/bf02269564>, 2002.

1111 Schiebel, R., Spielhagen, R. F., Garnier, J., Hagemann, J., Howa, H., Jentzen, A., Martínez-García, A., Meilland, J., Michel,

1112 E., and Repschläger, J.: Modern planktic foraminifers in the high-latitude ocean, *Marine Micropaleontology*, 136, 1–13,

1113 <https://doi.org/10.1016/j.marmicro.2017.08.004>, 2017.

1114 Schlüter, L., Lohbeck, K. T., Gutowska, M. A., Gröger, J. P., Riebesell, U., and Reusch, T. B.: Adaptation of a globally

1115 important coccolithophore to ocean warming and acidification, *Nature Climate Change*, 4, 1024–1030,

1116 <https://doi.org/10.1038/nclimate2379>, 2014.

1117 Sinha, B., Buitenhuis, E. T., Le Quéré, C., and Anderson, T. R.: Comparison of the emergent behavior of a complex ecosystem

1118 model in two ocean general circulation models, *Progress in Oceanography*, 84, 204–224,

1119 <https://doi.org/10.1016/j.pocean.2009.10.003>, 2010.

1120 Smith, S. V. and Mackenzie, F. T.: The role of CaCO₃ reactions in the contemporary oceanic CO₂ cycle, *Aquatic Geochemistry*,

域代码已更改

22, 153–175, <https://doi.org/10.1007/s10498-015-9282-y>, 2016.

Steiner, Z., Turehyn, A. V., Harpaz, E., and Silverman, J.: Water chemistry reveals a significant decline in coral calcification rates in the southern Red Sea, *Nature communications*, 9, 3615, <https://doi.org/10.1038/s41467-018-06030-6>, 2018.

Subhas, A. V., Rollins, N. E., Berelson, W. M., Erez, J., Ziveri, P., Langer, G., and Adkins, J. F.: The dissolution behavior of biogenic calcites in seawater and a possible role for magnesium and organic carbon, *Marine Chemistry*, 205, 100–112, <https://doi.org/10.1016/j.marchem.2018.08.001>, 2018.

Subhas, A. V., Dong, S., Naviaux, J. D., Rollins, N. E., Ziveri, P., Gray, W., Rae, J. W., Liu, X., Byrne, R. H., and Chen, S.: Shallow calcium carbonate cycling in the North Pacific Ocean, *Global Biogeochemical Cycles*, 36, e2022GB007388, <https://doi.org/10.7185/gold2021.4474>, 2022.

Sulpis, O., Jeansson, E., Dinuer, A., Lauvset, S. K., and Middelburg, J. J.: Calcium carbonate dissolution patterns in the ocean, *Nature Geoscience*, 14, 423–428, <https://doi.org/10.1038/s41561-021-00743-y>, 2021.

Takahashi, T., Sutherland, S. C., Wanninkhof, R., Sweeney, C., Feely, R. A., Chipman, D. W., Hales, B., Friederich, G., Chavez, F., and Sabine, C.: Climatological mean and decadal change in surface ocean $p\text{CO}_2$, and net sea–air CO_2 flux over the global oceans, *Deep Sea Research II*, 56, 554–577, <https://doi.org/10.1016/j.dsr2.2008.12.009>, 2009.

Volk, T. and Hoffert, M. I.: Ocean carbon pumps: Analysis of relative strengths and efficiencies in ocean-driven atmospheric CO_2 changes, The carbon cycle and atmospheric CO_2 : Natural variations Archean to present, 32, 99–110, <https://doi.org/10.1029/gm032p0099>, 1985.

White, M. M., Waller, J. D., Lubelezyk, L. C., Drapeau, D. T., Bowler, B. C., Balch, W. M., and Fields, D. M.: Coccolith dissolution within copepod guts affects fecal pellet density and sinking rate, *Scientific Reports*, 8, 9758, <https://doi.org/10.1038/s41598-018-28073-x>, 2018.

Wilson, R., Millero, F., Taylor, J., Walsh, P., Christensen, V., Jennings, S., and Grosell, M.: Contribution of fish to the marine inorganic carbon cycle, *Science*, 323, 359–362, <https://doi.org/10.1126/science.115797>, 2009.

Yang, T.-N. and Wei, K.-Y.: How many coccoliths are there in a coccosphere of the extant coccolithophorids? A compilation, *Br. Phycol. J.*, 26, 67–80, <https://doi.org/10.58998/jnr2275>, 2003.

Cocciobiom2 — Macros, — available — at: — ina.tmsoc.org/nannos/cocciobiom/Usernotes.html:

<http://ina.tmsoc.org/nannos/ecccobiom/Usernotes.html>

Young, J. R. and Ziveri, P.: Calculation of coccolith volume and its use in calibration of carbonate flux estimates, *Deep-sea research II*, 47, 1679-1700, [https://doi.org/10.1016/S0967-0645\(00\)00003-5](https://doi.org/10.1016/S0967-0645(00)00003-5), 2000.

Ziveri, P., de Bernardi, B., Baumann, K. H., Stoll, H. M., and Mortyn, P. G.: Sinking of coccolith carbonate and potential contribution to organic carbon ballasting in the deep ocean, *Deep-Sea Research Part II: Topical Studies in Oceanography*, 54, 659-675, <https://doi.org/10.1016/j.dsr2.2007.01.006>, 2007.

Ziveri, P., Gray, W. R., Anglada-Ortiz, G., Manno, C., Grelaud, M., Incarbona, A., Rae, J. W. B., Subhas, A. V., Pallaeks, S., and White, A.: Pelagic calcium carbonate production and shallow dissolution in the North Pacific Ocean, *Nature communications*, 14, 805, <https://doi.org/10.1038/s41467-023-36177-w>, 2023.